

Circulation Research

JOURNAL OF THE AMERICAN HEART ASSOCIATION



Increases in Mitochondrial Reactive Oxygen Species Trigger Hypoxia-Induced Calcium Responses in Pulmonary Artery Smooth Muscle Cells

Gregory B. Waypa, Robert Guzy, Paul T. Mungai, Mathew M. Mack, Jeremy D. Marks, Michael W. Roe and Paul T. Schumacker

Circ. Res. 2006;99:970-978; originally published online Sep 28, 2006;

DOI: 10.1161/01.RES.0000247068.75808.3f

Circulation Research is published by the American Heart Association. 7272 Greenville Avenue, Dallas, TX 75214

Copyright © 2006 American Heart Association. All rights reserved. Print ISSN: 0009-7330. Online ISSN: 1524-4571

The online version of this article, along with updated information and services, is located on the World Wide Web at:

<http://circres.ahajournals.org/cgi/content/full/99/9/970>

Data Supplement (unedited) at:

<http://circres.ahajournals.org/cgi/content/full/01.RES.0000247068.75808.3f/DC1>

Subscriptions: Information about subscribing to Circulation Research is online at
<http://circres.ahajournals.org/subscriptions/>

Permissions: Permissions & Rights Desk, Lippincott Williams & Wilkins, a division of Wolters Kluwer Health, 351 West Camden Street, Baltimore, MD 21202-2436. Phone: 410-528-4050. Fax: 410-528-8550. E-mail:
jurnalpermissions@lww.com

Reprints: Information about reprints can be found online at
<http://www.lww.com/reprints>

Increases in Mitochondrial Reactive Oxygen Species Trigger Hypoxia-Induced Calcium Responses in Pulmonary Artery Smooth Muscle Cells

Gregory B. Waypa, Robert Guzy, Paul T. Mungai, Mathew M. Mack, Jeremy D. Marks,
Michael W. Roe, Paul T. Schumacker

Abstract—Mitochondria have been implicated as a potential site of O₂ sensing underlying hypoxic pulmonary vasoconstriction (HPV), but 2 disparate models have been proposed to explain their reaction to hypoxia. One model proposes that hypoxia-induced increases in mitochondrial reactive oxygen species (ROS) generation activate HPV through an oxidant-signaling pathway, whereas the other proposes that HPV is a result of decreased oxidant signaling. In an attempt to resolve this debate, we use a novel, ratiometric, redox-sensitive fluorescence resonance energy transfer (HSP-FRET) probe, in concert with measurements of reduced/oxidized glutathione (GSH/GSSG), to assess cytosolic redox responses in cultured pulmonary artery smooth muscle cells (PASMCs). Superfusion of PASMCs with hypoxic media increases the HSP-FRET ratio and decreases GSH/GSSG, indicating an increase in oxidant stress. The antioxidants pyrrolidinedithiocarbamate and N-acetyl-L-cysteine attenuated this response, as well as the hypoxia-induced increases in cytosolic calcium ([Ca²⁺]_i), assessed by the Ca²⁺-sensitive FRET sensor YC2.3. Adenoviral overexpression of glutathione peroxidase or cytosolic or mitochondrial catalase attenuated the hypoxia-induced increase in ROS signaling and [Ca²⁺]_i. Adenoviral overexpression of cytosolic Cu, Zn-superoxide dismutase (SOD-I) had no effect on the hypoxia-induced increase in ROS signaling and [Ca²⁺]_i, whereas mitochondrial matrix-targeted Mn-SOD (SOD-II) augmented [Ca²⁺]_i. The mitochondrial inhibitor myxothiazol attenuated the hypoxia-induced changes in the ROS signaling and [Ca²⁺]_i, whereas cyanide augmented the increase in [Ca²⁺]_i. Finally, simultaneous measurement of ROS and Ca²⁺ signaling in the same cell revealed that the initial increase in these 2 signals could not be distinguished temporally. These results demonstrate that hypoxia triggers increases in PASMC [Ca²⁺]_i by augmenting ROS signaling from the mitochondria. (*Circ Res*. 2006;99:970-978.)

Key Words: hypoxic pulmonary vasoconstriction ■ reactive oxygen species ■ redox signaling ■ antioxidants
■ fluorescence resonance energy transfer

Although hypoxic pulmonary vasoconstriction (HPV) was first described by von Euler and Liljestrand in 1946,¹ the underlying mechanism by which vascular cells detect the decrease in O₂ tension has not been established. Hypoxia activates an O₂ sensor that triggers contraction of pulmonary artery smooth muscle cells (PASMCs) through an increase in cytosolic calcium ([Ca²⁺]_i) via release of Ca²⁺ from the sarcoplasmic reticulum and/or entry of extracellular Ca²⁺ through voltage-, receptor-, or store-operated channels in the sarcolemma.²⁻⁸ However, the signaling pathways that couple the O₂ sensor to the increases in [Ca²⁺]_i have not been established.

Mitochondria have long been considered putative sites of oxygen sensing because they consume O₂ and therefore represent the intracellular site with the lowest oxygen tension.

Two opposing views have emerged regarding the nature of the O₂ sensor and the hypoxia signal transduction pathway. One model is based on measurements of reactive oxygen species (ROS) using lucigenin or luminol chemiluminescence in perfused lungs⁹ and more recent studies using chemiluminescence, Amplex Red, and 2',7'-dichlorodihydrofluorescein (DCF) in endothelium-denuded rings of distal pulmonary artery (PA).¹⁰ Those studies reported finding a decrease in ROS levels during transition from normoxia to hypoxia, leading the authors to hypothesize that decreases in ROS produce a transition in cytosolic redox to a more reduced state.¹¹ This cytosolic reduction has been proposed to close redox-sensitive voltage-dependent potassium (K_v) channels in the plasma membrane, thereby depolarizing the membrane and allowing influx of Ca²⁺ through voltage-dependent

Original received September 7, 2005; resubmission received August 14, 2006; revised resubmission received September 11, 2006; accepted September 14, 2006.

From the Department of Pediatrics (G.B.W., R.G., P.T.M., P.T.S.), Division of Neonatology, Northwestern University, Chicago; Department of Pediatrics (J.D.M.), Section of Neonatology, and Department of Medicine (M.W.R., M.M.M.), Pulmonary and Critical Care Section (M.M.M.), The University of Chicago, Ill.

Correspondence to Gregory B. Waypa, Department of Pediatrics, Northwestern University, Ward Bldg 12-189, 303 E Chicago Ave, Chicago, IL 60611. E-mail g-waypa@northwestern.edu

© 2006 American Heart Association, Inc.

Circulation Research is available at <http://circres.ahajournals.org>

DOI: 10.1161/01.RES.0000247068.75808.3F

L-type Ca^{2+} channels. In support of their model, pharmacological reducing agents were found to cause constriction in isolated PA, whereas oxidizing agents produced relaxation.¹²

An alternate hypothesis is that hypoxia increases ROS generation in PASMCs. This response has been observed in earlier chemiluminescence and DCF fluorescence studies.^{13–15} Other studies have also detected increases in oxidant production during hypoxia using lucigenin-derived chemiluminescence and electron paramagnetic resonance (EPR) spectrometry.¹⁶ The hypoxia-induced increase in oxidants is hypothesized to trigger an increase in $[\text{Ca}^{2+}]_i$, resulting in PASMC contraction.¹⁷ In support of that model, chemically dissimilar antioxidants or overexpression of catalase block the HPV response,^{14,16,17} whereas exogenous H_2O_2 mimics HPV in PASMCs and isolated lungs.^{14,17}

Experimental resolution of the question of whether ROS levels increase or decrease during hypoxia has been problematic because of the technical limitations of the tools used to assess oxidant stress. Fluorescent probes such as DCF and dihydroethidium lack specificity¹⁸ and can accumulate within organelles. Similarly, autoxidation and limited intracellular access interfere with the ability of lucigenin or luminol to detect intracellular oxidants.¹⁹ Moreover, none of these probes exhibits ratiometric fluorescence, so that a change in intracellular dye concentration or fluorescence path length caused by a change in cell volume will alter fluorescence intensity unrelated to changes in ROS. To address this problem, we assessed cellular redox responses to hypoxia using a ratiometric, redox-sensitive protein sensor, HSP-FRET, expressed in cultured rat PASMCs. This sensor consists of enhanced cyan (CFP) and yellow (YFP) fluorescent protein motifs linked by the redox-dependent regulatory domain from the bacterial heat shock protein HSP-33.²⁰ The HSP-33 domain contains 4 highly conserved cysteine residues coordinating a zinc binding domain. Oxidation of the thiols leads to release of zinc and the formation of 2 disulfides,²¹ resulting in a structural change in the optical coupling of CFP and YFP. When expressed in cells, this protein provides a sensitive, real-time assessment of changes in redox conditions in the cytosol.²² These studies were complemented with measurements of cellular reduced/oxidized glutathione (GSH/GSSG), which provides an independent assessment of changes in cellular redox balance.

These studies demonstrate that hypoxia triggers an increase in mitochondrial ROS generation from the proximal region of the electron transport chain (ETC). The resulting oxidant stress activates a signal transduction cascade that is necessary and sufficient to cause an increase in cytosolic Ca^{2+} in PASMCs.

Materials and Methods

An expanded Materials and Methods section is available in the online data supplement at <http://circres.ahajournals.org>.

Pharmacological Agents and Adenoviruses

Endothelin-1 was obtained from American Peptide; rotenone, myxothiazol, cyanide, ammonium pyrrolidinedithiocarbamate (PDTC), and N-acetyl-L-cysteine (NAC) were obtained from Sigma. Cellular overexpression of enzymatic antioxidants was achieved using recombinant adenoviruses expressing cytosolic catalase and mitochondria

catalase,²³ as well as Cu, Zn-superoxide dismutase (SOD-I), Mn-SOD (SOD-II), and glutathione peroxidase (GPx1-c-Myc tagged).^{24–26}

Pulmonary Microvessel Myocyte Isolation

PASMCs were isolated from rat lungs as described previously¹⁴ using a modification of the method of Marshall et al.¹³ Cells isolated by this method were confirmed to be PAsMCs as previously described.¹⁴ All animals were housed and cared for under National Research Council guidelines for care and use of laboratory animals.

Measurements of GSH and GSSG

GSH and GSSG were measured in PASMCs using a Bioxytech GSH/GSSG-412 kit (Oxis Health Products Inc).

FRET Probes

The HSP-FRET probe was generated by inserting YFP into the pECFP-N1 plasmid (Clontech) between the *NheI* and *BglII* sites and then ligating the redox-sensitive regulatory domain from the *Escherichia coli* HSP-33 between YFP and CFP via the *EcoRI* and *BamHI* sites.²² Cells were placed into suspension by trypsinization, then transfected with HSP-FRET using an Amaxa Nucleofector device and plated on glass cover slips. HSP-FRET was excited at 430 nm, whereas fluorescence emission images were obtained at 470 nm (FRET donor, CFP) and 535 (FRET acceptor, YFP) to measure cell redox. Under reducing conditions, the CFP and YFP are in close proximity, and FRET is high. During oxidant stress, oxidation of thiols in the HSP-33 regulatory domain separates the fluorophores and decreases FRET. This increases image intensity at 470 and decreases intensity at 535 nm, resulting in an increase in the 470/535 HSP-FRET ratio.

A genetically encoded FRET-based sensor was used to measure $[\text{Ca}^{2+}]_i$. YC2.3 is a high-affinity Ca^{2+} sensor, consisting of CFP and citrine, a mutant of YFP linked by a calmodulin-M13 hinge region.^{27–29} When bound to Ca^{2+} , FRET between CFP and citrine increases. An increase in $[\text{Ca}^{2+}]_i$ is reflected by an increase in the citrine/CFP intensity ratio (535/470). The YC2.3 probe was determined to be unresponsive to exogenously applied oxidants (see the online data supplement). YC2.3 was packaged in a recombinant adenovirus to permit efficient expression of the probe in PASMCs.

Statistics

ANOVA was used to identify significant differences between groups. To control for differences in the hypoxic responses of cultured myocytes, experimental studies and control experiments were always performed on the same day. Statistical significance was set at $P < 0.05$.³⁰

Results

Hypoxia Shifts the Cytosol to a More Oxidized State

To assess the effects of hypoxia on cellular redox status, the ratio of GSH to GSSG was measured in cultured cells. PASMCs were subjected to hypoxia (2 hours at 1.5% O_2) in a glove-box, which permitted harvesting of cell lysates without reoxygenation. Hypoxia significantly decreased GSH/GSSG, indicating a shift in the glutathione pool to a more oxidized state (Figure 1). Exogenous H_2O_2 (20 $\mu\text{mol/L}$, 15 minutes) also decreased the GSH/GSSG ratio in normoxic cells. The mitochondrial inhibitor myxothiazol prevents electron entry into complex III, thereby preventing ROS generation from complex III or IV. Myxothiazol (100 nmol/L) attenuated the hypoxia-induced decrease in GSH/GSSG without affecting decrease induced by H_2O_2 . These results indicate that hypoxia decreases the ratio of reduced to oxidized

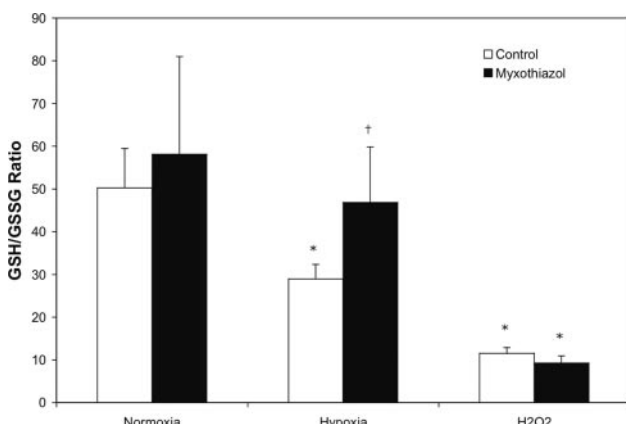


Figure 1. Cytosolic ratio of GSH to GSSG in PASMCs after 2 hours of exposure to hypoxia (1.5% O₂). Myxothiazol (100 nmol/L) was administered to inhibit electron flux into complex III. Values are means \pm SE ($n=8$ dishes). * $P<0.05$ compared with normoxic control, † $P<0.05$ compared with hypoxic control.

glutathione and that this oxidant stress requires electron transport into mitochondrial complex III.

Changes in ROS Signaling and Cytosolic Calcium
 PASMCs transfected with the HSP-FRET exhibited a uniform pattern of confocal fluorescence (Figure 2A) that was indistinguishable in appearance from the pattern observed in cells transfected with a nontargeted green fluorescence protein (GFP) expression vector (Clontech EGFP-N1) (see the online data supplement). Although confocal images of PASMCs transduced with YC2.3 exhibited some fluorescence in the nucleus, most of the distribution of the probe was cytosolic (Figure 2E). These images were obtained using excitation laser line at 488 nm and emission at 535 nm. Separate excitation images were obtained for CFP and YFP components of HSP-FRET to confirm colocalization of the fluorophores in PASMCs (see the online data supplement). Individual PASMCs expressing HSP-FRET were imaged every 60 seconds. After establishing a stable baseline under normoxia, the gas bubbling the media was switched to hypoxia (1.5% O₂). This elicited an increase in the CFP fluorescence intensity (Figure 2B), a decrease in the YFP fluorescence intensity (Figure 2C), and an increase in the CFP/YFP ratio (Figure 2D) within 3 to 5 minutes, indicating oxidation of the sensor. Individual PASMCs expressing YC2.3 were imaged every 10 seconds. When cells were exposed to hypoxia, citrine fluorescence increased (Figure 2F) and CFP fluorescence decreased (Figure 2G), producing an increase in citrine/CFP ratio (Figure 2H), which was indicative of an increase in [Ca²⁺]_i. Results were summarized by determining the peak increase in HSP-FRET and YC2.3 ratios.

To determine the contribution of ROS to the HSP-FRET and YC2.3 responses, PASMCs were treated with antioxidants. The hypoxia-induced increase in HSP-FRET ratio was significantly attenuated by PDTC (10 μ mol/L) and by NAC (0.5 mmol/L) as was the hypoxia-induced [Ca²⁺]_i increase (Figure 3). PDTC and NAC had no effect on baseline HSP-FRET or YC2.3 ratios during normoxia (see the online data supplement). To assess the role of mitochondrial electron transport, PASMCs were treated with myxothiazol to inhibit complex III or cyanide to inhibit complex IV. Myxothiazol

(10 μ mol/L) significantly attenuated the hypoxia-induced HSP-FRET and YC2.3 responses, whereas cyanide (1 μ mol/L) failed to prevent the increased cytosolic oxidation and augmented [Ca²⁺]_i during hypoxia. Myxothiazol and cyanide had no effect on baseline HSP-FRET or YC2.3 ratios during normoxia (see the online data supplement). Taken together, the results suggest that a cytosolic oxidant signal triggers an increase in [Ca²⁺]_i during hypoxia and that electron flux into complex III is required for the cytosolic oxidant signal, whereas electron transport through complex IV is not necessary.

Cellular Overexpression of Antioxidant Enzymes Selectively Inhibit HPV

To further assess the role of ROS signaling in HPV, glutathione peroxidase (GPx1) was overexpressed in PASMCs. Western blot analysis for the c-Myc-tagged GPx1 protein revealed dose-dependent expression of GPx1 (Figure 4, inset). GPx1 (5 pfu) significantly decreased the hypoxia-induced increase HSP-FRET oxidation (Figure 4), along with the increase in [Ca²⁺]_i as assessed by YC2.3, although not as effectively as the pharmacological antioxidants.

To further explore the relationship between hypoxia-induced ROS signaling and the increase in [Ca²⁺]_i, catalase was overexpressed in the cell or the mitochondrial matrix in PASMCs (Figure 5A). Laser-scanning confocal images confirmed the proper targeting of the proteins (Figure 5B through 5D). Both cytosolic and mitochondrial catalase overexpression attenuated the hypoxia-induced increase in both cytosolic oxidant signaling and [Ca²⁺]_i as assessed by the HSP-FRET and YC2.3 responses, respectively (Figure 6). Coexpression of cytosolic and mitochondrial catalase was not more effective than either agent alone (see the online data supplement). This suggests that H₂O₂ signaling in both cytosol and matrix compartments may contribute to the hypoxia-induced increase in [Ca²⁺]_i. Similarly, SOD-I and SOD-II were overexpressed in PASMCs, and expression levels and targeting were determined by immunoblotting (Figure 5A) and confocal microscopy, respectively (Figure 5E through 5J). Overexpression of SOD-I had no significant effect on either the hypoxia-induced oxidant signaling or [Ca²⁺]_i response to hypoxia, whereas overexpression of SOD-II significantly augmented the [Ca²⁺]_i response but, like SOD I, had no effect on the hypoxia-induced oxidant signaling (Figure 6). These results suggest that the HSP-FRET probe is not responsive to superoxide and that superoxide production leading to H₂O₂ in the mitochondria contributes to the hypoxia-induced increase in [Ca²⁺]_i.

Simultaneous Comparison of ROS and Calcium Signaling

Assessment of [Ca²⁺]_i and ROS signals in the same cell using HSP-FRET and YC2.3 is precluded by their common use of CFP and YFP. We therefore used Fura-2 to assess [Ca²⁺]_i and HSP-FRET to assess redox signaling in the same cells. Fluorescence images for the 2 sensors were alternated, and three sets of ratiometric measurements were collected every 20 seconds. This provided a virtually simultaneous assessment of calcium and redox responses in the same cells. Ratiometric images were

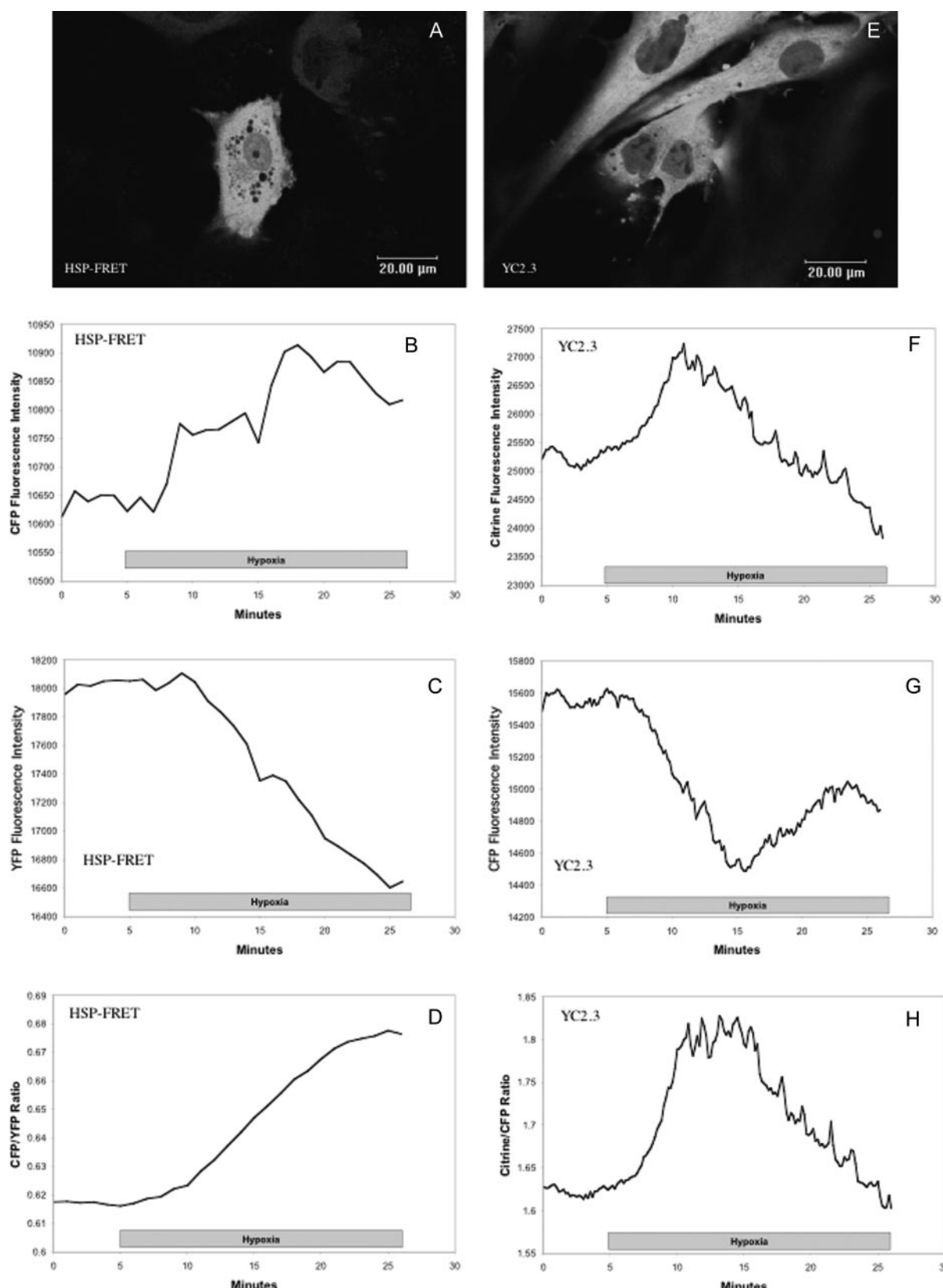


Figure 2. Effect of hypoxia on ROS signaling and $[Ca^{2+}]_i$ as assessed by the HSP-FRET and YC2.3 probes. Laser-scanning confocal images detailing expression of the FRET probes in PASMcs: HSP-FRET (A) and YC2.3 (E). Images were obtained using excitation at 488 nm and emission at 535 nm. Averaged responses of CFP fluorescence intensity (B), YFP fluorescence intensity (C), and HSP-FRET (CFP/YFP) ratio (D) in PASMcs ($n=23$) superfused with hypoxic (1.5% O₂) media. Averaged responses of citrine fluorescence intensity (F), CFP fluorescence intensity (G), and YC2.3 (citrine/CFP) ratio (H) in PASMcs ($n=17$) superfused with hypoxic (1.5% O₂) media.

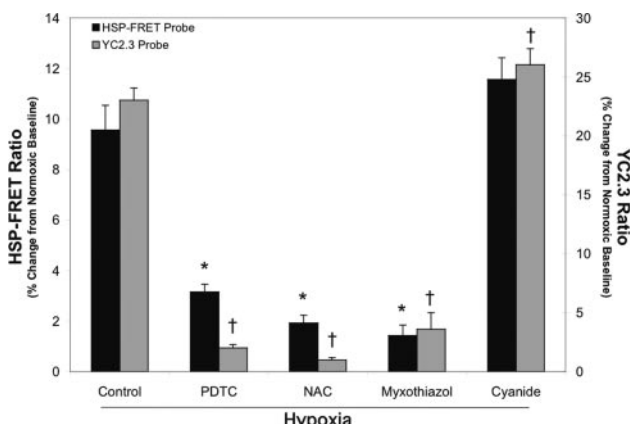


Figure 3. Effects of hypoxia on ROS signaling and $[Ca^{2+}]_i$ in PASMCs assessed by HSP-FRET and YC2.3, respectively. The antioxidants PDTC (10 $\mu\text{mol/L}$) or *N*-acetyl-L-cysteine (NAC) (0.5 mmol/L), or the mitochondrial inhibitors myxothiazol (10 $\mu\text{mol/L}$) or cyanide (1 $\mu\text{mol/L}$), were administered. Values are means \pm SE ($n=4$ cover slips). * $P<0.05$ compared with HSP-FRET hypoxic control. † $P<0.05$ compared with YC2.3 hypoxic control.

acquired during baseline, followed by 30 minutes of hypoxia (Figure 7). This analysis revealed that the initial increases in ROS and $[Ca^{2+}]_i$ could not be distinguished temporally. Although further increases in HSP-FRET ratios accumulated over time, these results do not refute the conclusion that the initial increase in calcium was triggered by ROS.

Discussion

This study extends prior work by demonstrating that hypoxia increases oxidant signaling in the cytosol of cultured PASMCs during hypoxia. Using HSP-FRET in parallel with measurements of GSH/GSSG to assess the redox state of the cell, we observed a shift toward a more oxidized state in PASMCs during hypoxia. The increase in oxidant signaling was attenuated by the antioxidants PDTC and NAC, which

act by reducing thiol groups and enhancing ROS scavenging. The oxidant signal was also attenuated by overexpression of GPx1, cytosolic catalase, or mitochondrial catalase, further supporting an involvement of H_2O_2 . The relationship between ROS signaling and the increase in $[Ca^{2+}]_i$ was explored using YC2.3, a FRET-based ratiometric Ca^{2+} sensor. Increases in $[Ca^{2+}]_i$ during hypoxia were attenuated by antioxidants, as well as by overexpression of GPx1 or cytosolic or mitochondrial catalase. Myxothiazol, an inhibitor of electron transport at complex III, inhibited the responses to hypoxia, suggesting the mitochondrial ETC is the source of the hypoxia-induced ROS signal. Cyanide, which inhibits at complex IV, increased the Ca^{2+} signal but did not prevent the oxidant signal. These findings indicate that a fully functional ETC is not required for the hypoxic response but that electron flux through complex III is required because it is the source of the increase in ROS responsible for triggering the increase in $[Ca^{2+}]_i$ during hypoxia in PASMCs. These findings support the hypothesis that mitochondria are required for O_2 sensing in HPV because of their ability to augment ROS signaling during hypoxia.

Increased ROS Signaling Triggers HPV

Our results do not support the proposed model in which hypoxia decreases the generation of ROS in PASMCs and shifts the cytosol to a more reduced state.^{2,9–11,31,32} According to that scheme, the decrease in oxidant signaling causes closure of redox-sensitive K_v channels,^{2,11} resulting in membrane depolarization and the opening of voltage-gated Ca^{2+} channels.^{2,31} Central to the contrast between that model and ours is the issue of whether oxidant stress in PASMCs increases or decreases during hypoxia. In that regard, some investigators have detected increases,^{14–16} whereas other studies find decreases.^{2,9,10} Resolution of this issue has been hindered by the lack of a ratiometric sensor capable of detecting changes in the redox status of thiol-containing proteins in live cells. Using HSP-FRET, the conformation of which is regulated by a redox-sensitive HSP-33 domain, we now find evidence of protein thiol oxidation during hypoxia. Because the expression of HSP-FRET is predominantly within the cytosol, these findings indicate that oxidant signaling must occur in that compartment.

The hypoxia-induced increase in oxidant stress detected with HSP-FRET is consistent with the measured decrease in GSH/GSSG, although the latter responded more slowly than did the former, which began to change within minutes. It seems likely that endogenous glutathione reductase would defend against decreases in GSH/GSSG, thereby delaying the appearance of changes in that ratio. By contrast, refolding of HSP-FRET appears to occur slowly (data not shown), so changes in the oxidation state of HSP-FRET molecules could accumulate more rapidly and allow earlier detection. Both responses are consistent with the observation that chemical antioxidants and overexpression of oxidant scavenging proteins attenuate both the oxidant signal and the downstream calcium response to hypoxia. The involvement of a hypoxia-induced ROS signal is further supported by the observation that exogenous H_2O_2 mimics HPV in PASMCs and in isolated lungs.^{14,17}

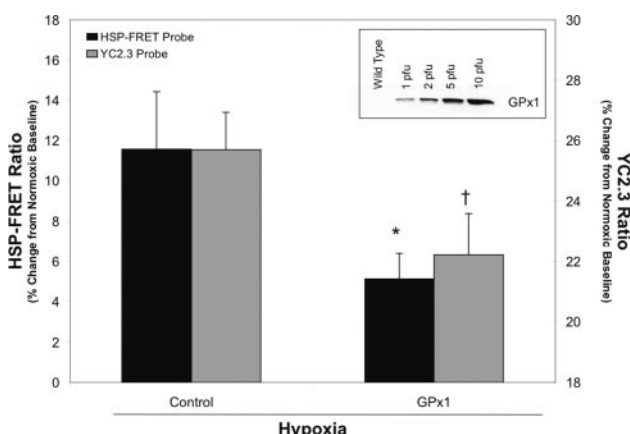


Figure 4. Effects of glutathione peroxidase (GPx1) on the responses to hypoxia. Response of GPx1 (5 pfu) overexpression in PASMC on hypoxia-induced increases in HSP-FRET and YC2.3. Inset, Western blot analysis for the c-Myc-tagged GPx1 illustrates overexpression of GPx1 in PASMCs. Values are means \pm SE ($n=4$ cover slips). * $P<0.05$ compared with HSP-FRET hypoxic control. † $P<0.05$ compared with YC2.3 hypoxic control.

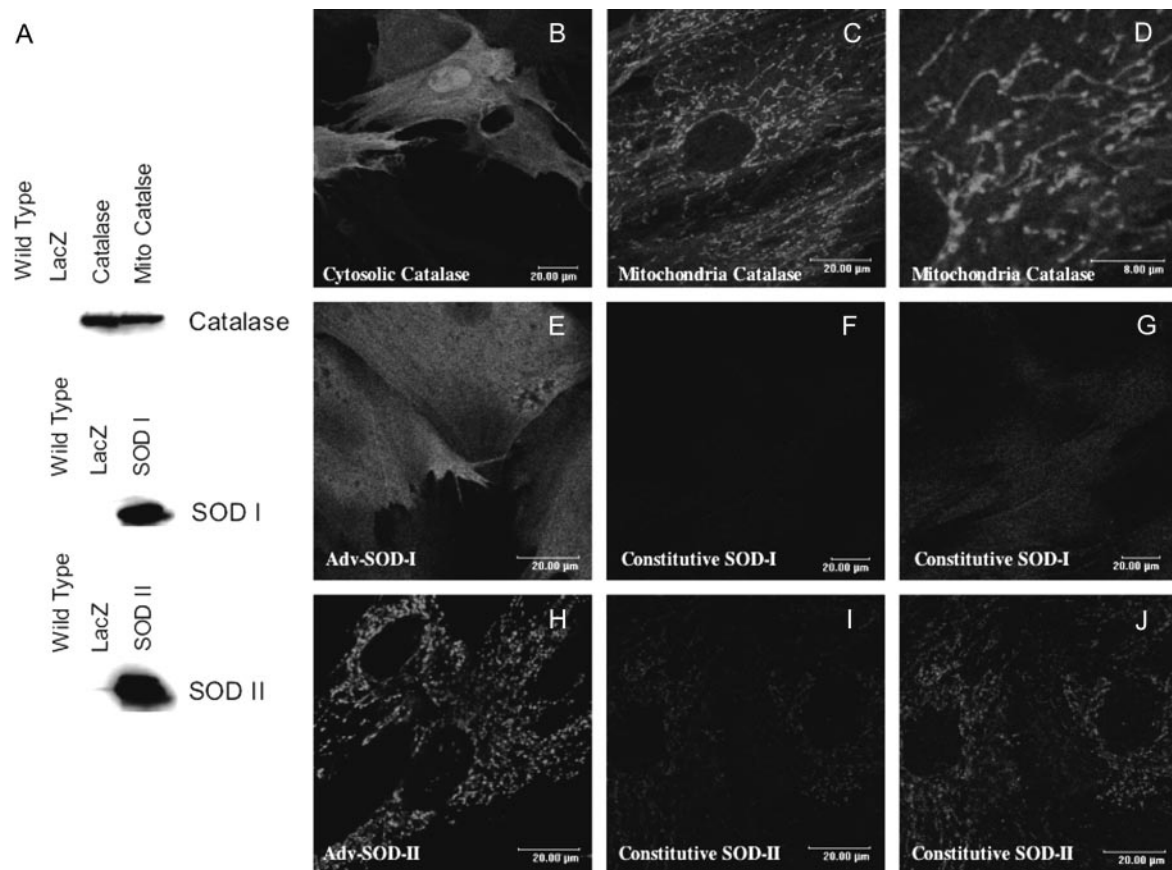


Figure 5. Expression of targeted enzymatic antioxidants. A, Western blots for catalase, mitochondrial catalase, SOD-I, and SOD-II overexpression in PASMcs. B, Cytosolic catalase. C, Mitochondrial catalase. D, High magnification of image in C. E, Overexpression of SOD-I in PASMcs. F, Constitutive SOD-I expression in control cells using similar gain as E. G, Constitutive SOD-I expression in control cells using high gain. H, Overexpression of mitochondrial targeted SOD-II in PASMcs. I, Constitutive SOD-II expression in control cells using similar gain as H. J, Constitutive SOD-II expression in control cells using high gain.

ROS Signaling and Increases in $[Ca^{2+}]_i$

Although ratiometric sensors such as Fura-2 are available for assessing $[Ca^{2+}]_i$, the accumulation of these probes in mitochondria and other organelles can interfere with their ability to

provide a measure of Ca^{2+} in the cytosol.³³ To address this limitation we used a Ca^{2+} -sensitive, ratiometric FRET sensor (YC2.3) to measure changes in Ca^{2+} signaling in PASMcs.²⁹ YC2.3 was expressed in the cytosol, and its property as a

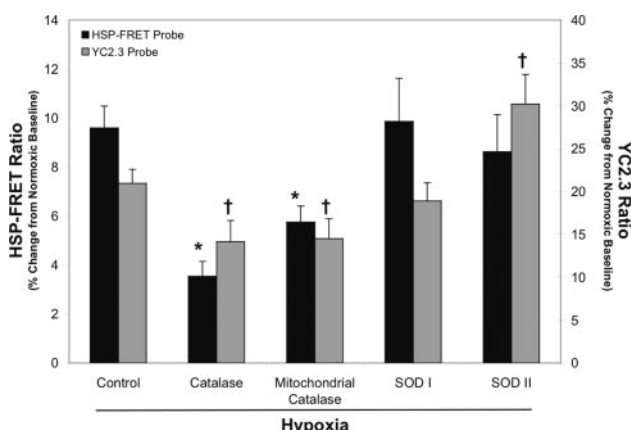


Figure 6. Effects of hypoxia on ROS signaling and $[Ca^{2+}]_i$ in PASMcs assessed by HSP-FRET and YC2.3, respectively. In select experiments, the PASMcs were infected with recombinant adenovirus containing catalase, mitochondrial catalase, SOD-I, or SOD-II. Values are means \pm SE ($n=4$ cover slips). * $P<0.05$ compared with HSP-FRET hypoxic control. † $P<0.05$ compared with YC2.3 hypoxic control.

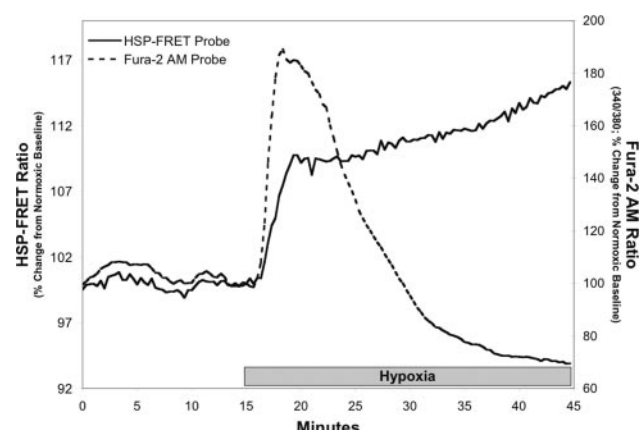


Figure 7. Simultaneous measurement of HSP-FRET ratio and Fura-2 ratio in PASMcs, to assess, respectively, the temporal relationship between ROS signaling and the increase in $[Ca^{2+}]_i$ triggered by hypoxia. No difference in the initial increase in these signals was detectable. Lines represent the average HSP-FRET and Fura-2 ratios for 4 cover slips containing 4 to 8 cells each.

high-affinity sensor of Ca^{2+} permits assessment of signals in that compartment.^{27–29}

Many studies have shown that PASMC contraction during hypoxia results from an increase in $[\text{Ca}^{2+}]_i$.^{3,4,6,8,31} The present study extends that work by showing a connection between hypoxia-induced increases in ROS signaling and $[\text{Ca}^{2+}]_i$ in PASMCs. Both PDTc and NAC attenuated the hypoxia-induced increase in $[\text{Ca}^{2+}]_i$, as did overexpression of the antioxidant proteins GPx1 and catalase, consistent with previous studies.¹⁷ Mitochondria-targeted catalase also attenuated the response, which suggests that H_2O_2 arising from the mitochondria is important for triggering increases in $[\text{Ca}^{2+}]_i$ during HPV. However, overexpression of catalase in the mitochondria could conceivably enhance the scavenging of oxidants originating in the cytosol, so this result should be interpreted with caution. We note that the pharmacological antioxidants were more effective at attenuating the responses than were the enzymatic antioxidants. This may be attributable to an ability of the pharmacological agents to access subcellular compartments that the protein antioxidants cannot reach. Moreover, pharmacological antioxidants can act both to scavenge ROS and to chemically reduce the cellular targets of those oxidant signals, producing a more effective attenuation of the downstream response than with ROS scavengers alone.

Overexpression of SOD-II enhanced the $[\text{Ca}^{2+}]_i$ response to hypoxia. Because SOD-II expression is limited to the matrix compartment, these results strengthen the conclusion that H_2O_2 arising from that compartment contributes to HPV. However, Rodríguez et al observed that SOD-II overexpression in the mitochondrial matrix of HT-1080 fibrosarcoma cells caused an increase in H_2O_2 production through an unknown mechanism unrelated to its SOD activity.³⁴ Such a paradoxical increase in oxidant production by SOD-II might explain why $[\text{Ca}^{2+}]_i$ responses were augmented by overexpression of SOD-II in our study. Nevertheless, we did not find evidence of an elevated normoxic $[\text{Ca}^{2+}]_i$ that might have been expected if basal levels of ROS production had been accelerated. In either case, our findings reveal that H_2O_2 arising from mitochondria contributes to the hypoxic response, consistent with previous reports showing that antioxidants block the response to hypoxia in intact lungs, in isolated PA vessels, and in PASMCs.^{14,16,17} Our results are not consistent with the conclusions by Olszewski et al, who showed that exogenous reducing or oxidizing agents caused contraction or relaxation of PA vessels in accordance with their model of decreased ROS production in hypoxia.¹² The basis for these contradictory findings is unclear but may relate to the high concentrations of reducing or oxidizing agents used in their study, which may have affected multiple redox-sensitive targets in the cell.

Ours is the first study to compare the time course of ROS signaling (HSP-FRET) and the $[\text{Ca}^{2+}]_i$ response (Fura-2) in the same PASMCs during hypoxia. Within the resolution limits of these methods, there was no detectable difference in the time at which both signals began to increase. Because one signal did not clearly increase before the other, these results do not reveal whether one signal triggers the other or not. However, they do demonstrate a clear temporal association between the signals, and they do not exclude the possibility that ROS may have

triggered the initial increase in cytosolic calcium. The observation that antioxidant agents and targeted antioxidant proteins attenuate the ROS response and the calcium response indicates that ROS are required for the increase in $[\text{Ca}^{2+}]_i$ during hypoxia in PASMCs.

Mitochondrial Electron Transport and the Source of ROS During Hypoxia

Previous studies suggest that HPV requires electron transport in the proximal but not the distal region of the ETC.^{14,17,35,36} For example, inhibition of complex I by rotenone or diphenylene iodonium abrogates HPV,^{14,17,36} whereas inhibitors acting at more distal sites in the ETC, such as cyanide or antimycin A, fail to inhibit the response. This indicates that a fully functional ETC is not required for HPV,^{14,17,35} and it supports the observation that hypoxia-induced changes in [ATP] do not mediate HPV.³⁷ Myxothiazol inhibits the binding of ubiquinol at complex III, thereby preventing the oxidation of ubiquinol and the formation of ubisemiquinone. We find that myxothiazol attenuates the hypoxia-induced increase in oxidant stress and the associated increase in $[\text{Ca}^{2+}]_i$, which underscores the likely role of ubisemiquinone as a source of electrons responsible for superoxide generation, H_2O_2 production, and the subsequent increase in calcium. An earlier study reported that myxothiazol induces H_2O_2 production in isolated heart mitochondria under normoxia,³⁸ which complicates our interpretation of its effects on ROS generation. We did not detect an increase in ROS production with myxothiazol during normoxia, either in the form of a decrease in GSH/GSSG or by the HSP-FRET sensor. This may be attributable to differences in isolated mitochondria versus whole cells. Future studies with genetic tools will be useful in resolving this issue definitively. Cyanide had no effect on the hypoxia-induced increase in ROS, and it augmented the hypoxia-induced increase in $[\text{Ca}^{2+}]_i$. Because complex IV acts in series with complex III, one might expect cyanide to block electron transport through complex III by preventing electron flux from complex III to cytochrome c. Conceivably, electron leak pathways from cytochrome c to alternate targets, such as p66^{Shc},³⁹ would permit continued superoxide production at complex III during cyanide treatment, thus maintaining ROS generation during hypoxia.⁴⁰ That each of these mitochondrial inhibitors increases the cytosolic NAD(P)/NAD(P)H ratio, whereas only the proximal inhibitors block HPV, supports the view that changes in the NAD(P)/NAD(P)H couple are not responsible for signaling hypoxia in HPV hypoxia.³¹

The mechanism by which hypoxia augments ROS signaling from the electron transport chain under conditions of hypoxia remains unresolved. Three potential mechanisms have been proposed.⁴¹ The “Vectoral Transport” hypothesis suggests that hypoxia may increase the relative release of ROS from complex III toward the intermembrane space, while decreasing the relative release toward the matrix. The “Semiquinone Lifetime” hypothesis suggests that a decrease in O_2 interaction with protein or lipids at complex III could prolong the lifetime of ubisemiqui-

none at complex III. Finally, the "Oxygen Access" hypothesis suggests that hypoxia might increase the access of O₂ to semiquinone radical moiety at complex III. In each of these mechanisms, membrane O₂ levels would affect lipid-protein structure so as to increase electron transfer from ubisemiquinone to O₂, yielding an increase in superoxide release to the cytosol despite a decrease in the availability of oxygen.

Oxidation of HSP-FRET during hypoxia has recently been observed in other cell types, where hypoxia-induced, mitochondrial ROS signaling was shown to trigger stabilization of the hypoxia-inducible transcription factor (HIF).^{22,40} HPV is an acute response mediated by post-translational mechanisms, yet it also involves an increase in the generation of ROS by the mitochondria. Collectively, these observations suggest that the mitochondrial oxygen sensor is capable of triggering a wide range of responses to hypoxia in diverse cell types. Conceivably, tissue-specific responses to hypoxia could be regulated by the expression of redox-regulated signaling molecules capable of activating the cell-specific responses to the same upstream oxidant release from the mitochondria. Future studies are required to fully address this hypothesis.

Acknowledgments

We thank Dr Jingxiang Bai (Mount Sinai School of Medicine, New York) for providing recombinant adenoviruses containing Lac Z, catalase, and mitochondria-targeted catalase; Dr Christopher Rhodes (Pacific Northwest Research Institute, Seattle, Wash) for the adenovirus expressing YC2.3; and the University of Iowa Viral Vector Core for the adenoviruses expressing SOD-I, SOD-II, and GPx1. The HSP-FRET sensor was contributed by Drs Beatrice Hoyos and Ulrich Hammerling (Memorial Sloan-Kettering Cancer Center, New York). We also thank Dr Hong Chen and Chan Boriboun for technical assistance.

Sources of Funding

Supported by NIH grants HL66315, HL35440, and HL079650 (to P.T.S); American Heart Association Grant 0235457Z (to G.B.W.); and NIH/NIDDK DK63493 and a Research Grant from the American Diabetes Association (to M.W.R.).

Disclosures

None.

References

- von Euler U, Liljestrand G. Observations on the pulmonary arterial blood pressure of the cat. *Acta Physiol Scand*. 1946;12:301–320.
- Archer SL, Soul E, Dinh-Xuan AT, Schremmer B, Mercier JC, El Yaagoubi A, Nguyen-Huu L, Reeve HL, Hampl V. Molecular identification of the role of voltage-gated K⁺ channels, Kv1.5 and Kv2.1, in hypoxic pulmonary vasoconstriction and control of resting membrane potential in rat pulmonary artery myocytes. *J Clin Invest*. 1998;101:2319–2330.
- Dipp M, Nye PC, Evans AM. Hypoxic release of calcium from the sarcoplasmic reticulum of pulmonary artery smooth muscle. *Am J Physiol Lung Cell Mol Physiol*. 2001;281:L318–L325.
- Morio Y, McMurry IF. Ca(2+) release from ryanodine-sensitive store contributes to mechanism of hypoxic vasoconstriction in rat lungs. *J Appl Physiol*. 2002;92:527–534.
- Snetkov VA, Aaronson PI, Ward JP, Knock GA, Robertson TP. Capacitative calcium entry as a pulmonary specific vasoconstrictor mechanism in small muscular arteries of the rat. *Br J Pharmacol*. 2003;140:97–106.
- Wang J, Shimoda LA, Sylvester JT. Capacitative calcium entry and TRPC channel proteins are expressed in rat distal pulmonary arterial smooth muscle. *Am J Physiol Lung Cell Mol Physiol*. 2004;286:L848–L858.
- Sweeney M, Yuan JX. Hypoxic pulmonary vasoconstriction: role of voltage-gated potassium channels. *Respir Res*. 2000;1:40–48.
- Robertson TP, Hague D, Aaronson PI, Ward JP. Voltage-independent calcium entry in hypoxic pulmonary vasoconstriction of intrapulmonary arteries of the rat. *J Physiol London*. 2000;525(pt 3):669–80.
- Archer SL, Huang J, Henry T, Peterson D, Weir EK. A redox-based O₂ sensor in rat pulmonary vasculature. *Circ Res*. 1993;73:1100–1112.
- Michelakis ED, Hampl V, Nsair A, Wu X, Harry G, Haromy A, Gurtu R, Archer SL. Diversity in mitochondrial function explains differences in vascular oxygen sensing. *Circ Res*. 2002;90:1307–1315.
- Weir EK, Archer SL. The mechanism of acute hypoxic pulmonary vasoconstriction: the tale of two channels. *FASEB J*. 1995;9:183–189.
- Olszewski A, Hong Z, Peterson DA, Nelson DP, Porter VA, Weir EK. Opposite effects of redox status on membrane potential, cytosolic calcium, and tone in pulmonary arteries and ductus arteriosus. *Am J Physiol Lung Cell Mol Physiol*. 2004;286:L15–L22.
- Marshall C, Mamary AJ, Verhoeven AJ, Marshall BE. Pulmonary artery NADPH-oxidase is activated in hypoxic pulmonary vasoconstriction. *Am J Respir Cell Mol Biol*. 1996;15:633–644.
- Waypa GB, Chandel NS, Schumacker PT. Model for hypoxic pulmonary vasoconstriction involving mitochondrial oxygen sensing. *Circ Res*. 2001;88:1259–1266.
- Killilea DW, Hester R, Balczon R, Babal P, Gillespie MN. Free radical production in hypoxic pulmonary artery smooth muscle cells. *Am J Physiol Lung Cell Mol Physiol*. 2000;279:L408–L412.
- Liu JQ, Sham JS, Shimoda LA, Kuppusamy P, Sylvester JT. Hypoxic constriction and reactive oxygen species in porcine distal pulmonary arteries. *Am J Physiol Lung Cell Mol Physiol*. 2003;285:L322–L333.
- Waypa GB, Marks JD, Mack MM, Boriboun C, Mungai PT, Schumacker PT. Mitochondrial reactive oxygen species trigger calcium increases during hypoxia in pulmonary arterial myocytes. *Circ Res*. 2002;91:719–726.
- Thannickal VJ, Fanburg BL. Reactive oxygen species in cell signaling. *Am J Physiol Lung Cell Mol Physiol*. 2000;279:L1005–L1028.
- Spasovic I, Liochev SI, Fridovich I. Lucigenin: redox potential in aqueous media and redox cycling with O-(2) production. *Arch Biochem Biophys*. 2000;373:447–450.
- Janda I, Devedjiev Y, Derewenda U, Dauter Z, Bielnicki J, Cooper DR, Graf PC, Joachimiak A, Jakob U, Derewenda ZS. The crystal structure of the reduced, Zn2+-bound form of the *B. subtilis* Hsp33 chaperone and its implications for the activation mechanism. *Structure*. 2004;12:1901–1907.
- Barbirz S, Jakob U, Glocker MO. Mass spectrometry unravels disulfide bond formation as the mechanism that activates a molecular chaperone. *J Biol Chem*. 2000;275:18759–18766.
- Guzy RD, Hoyos B, Robin E, Chen H, Liu L, Mansfield KD, Simon MC, Hammerling U, Schumacker PT. Mitochondrial complex III is required for hypoxia-induced ROS production and cellular oxygen sensing. *Cell Metab*. 2005;1:401–408.
- Bai J, Cederbaum AI. Overexpression of catalase in the mitochondrial or cytosolic compartment increases sensitivity of HepG2 cells to tumor necrosis factor-alpha-induced apoptosis. *J Biol Chem*. 2000;275:19241–19249.
- Zwacka RM, Zhou W, Zhang Y, Darby CJ, Dudus L, Halldorson J, Oberley L, Engelhardt JF. Redox gene therapy for ischemia/reperfusion injury of the liver reduces AP1 and NF-kappaB activation. *Nat Med*. 1998;4:698–704.
- Zwacka RM, Dudus L, Epperly MW, Greenberger JS, Engelhardt JF. Redox gene therapy protects human IB-3 lung epithelial cells against ionizing radiation-induced apoptosis. *Hum Gene Ther*. 1998;9:1381–1386.
- Li Q, Sanlioglu S, Li S, Ritchie T, Oberley L, Engelhardt JF. GPx-1 gene delivery modulates NFkappaB activation following diverse environmental injuries through a specific subunit of the IKK complex. *Antioxid Redox Signal*. 2001;3:415–432.
- Miyawaki A, Llopis J, Heim R, McCaffery JM, Adams JA, Ikura M, Tsien RY. Fluorescent indicators for Ca2+ based on green fluorescent proteins and calmodulin. *Nature*. 1997;388:882–887.
- Miyawaki A, Griesbeck O, Heim R, Tsien RY. Dynamic and quantitative Ca2+ measurements using improved cameleons. *Proc Natl Acad Sci U S A*. 1999;96:2135–2140.
- Griesbeck O, Baird GS, Campbell RE, Zacharias DA, Tsien RY. Reducing the environmental sensitivity of yellow fluorescent protein. Mechanism and applications. *J Biol Chem*. 2001;276:29188–29194.
- Wallenstein S, Zucker CL, Fleiss JL. Some statistical methods useful in circulation research. *Circ Res*. 1980;47:1–9.

31. Archer SL, Weir EK, Reeve HL, Michelakis E. Molecular identification of O₂ sensors and O₂-sensitive potassium channels in the pulmonary circulation. *Adv Exp Med Biol.* 2000;475:219–240.
32. Moudgil R, Michelakis ED, Archer SL. Hypoxic pulmonary vasoconstriction. *J Appl Physiol.* 2005;98:390–403.
33. Wahl M, Sleight RG, Gruenstein E. Association of cytoplasmic free Ca²⁺ gradients with subcellular organelles. *J Cell Physiol.* 1992;150:593–609.
34. Rodríguez AM, Carrico PM, Mazurkiewicz JE, Meléndez JA. Mitochondrial or cytosolic catalase reverses the MnSOD-dependent inhibition of proliferation by enhancing respiratory chain activity, net ATP production, and decreasing the steady state levels of H(2)O(2). *Free Radic Biol Med.* 2000;29:801–813.
35. Leach RM, Hill HM, Snetkov VA, Robertson TP, Ward JP. Divergent roles of glycolysis and the mitochondrial electron transport chain in hypoxic pulmonary vasoconstriction of the rat: identity of the hypoxic sensor. *J Physiol London.* 2001;536:211–224.
36. Weissmann N, Ebert N, Ahrens M, Ghofrani HA, Schermuly RT, Hanze J, Fink L, Rose F, Conzen J, Seeger W, Grimminger F. Effects of mitochondrial inhibitors and uncouplers on hypoxic vasoconstriction in rabbit lungs. *Am J Respir Cell Mol Biol.* 2003;29:721–732.
37. Leach RM, Sheehan DW, Chacko VP, Sylvester JT. Energy state, pH, and vasomotor tone during hypoxia in precontracted pulmonary and femoral arteries. *Am J Physiol Lung Cell Mol Physiol.* 2000;278:L294–L304.
38. Starkov AA, Fiskum G. Myxothiazol induces H(2)O(2) production from mitochondrial respiratory chain. *Biochem Biophys Res Commun.* 2001;281:645–650.
39. Giorgio M, Migliaccio E, Orsini F, Paolucci D, Moroni M, Contursi C, Pelliccia G, Luzi L, Minucci S, Marcaccio M, Pinton P, Rizzuto R, Bernardi P, Paolucci F, Pelicci PG. Electron transfer between cytochrome c and p66^{Shc} generates reactive oxygen species that trigger mitochondrial apoptosis. *Cell.* 2005;122:221–233.
40. Chandel NS, Maltepe E, Goldwasser E, Mathieu CE, Simon MC, Schumacker PT. Mitochondrial reactive oxygen species trigger hypoxia-induced transcription. *Proc Natl Acad Sci U S A.* 1998;95:11715–11720.
41. Schumacker PT. Hypoxia-inducible factor-1 (HIF-1). *Crit Care Med.* 2005;33:S423–5.

Online Supplemental Data:

Methods

Pharmacological agents and adenoviruses. Endothelin-1 was obtained from American Peptide, and rotenone, myxothiazol, cyanide, ammonium pyrrolidinedithiocarbamate (PDTC) and N-acetyl-L-cysteine (NAC) were obtained from Sigma. Pharmacological agents were dissolved in DMSO (100%) as 1000x stock solutions so that when added to the media the DMSO concentration was 0.1%. Unless otherwise noted, these agents were incubated with the cells for 10 min prior to the start of the hypoxic challenge. Cellular overexpression of enzymatic antioxidants was achieved using recombinant adenoviruses expressing cytosolic catalase and mitochondria catalase [1], as well as Cu,Zn-superoxide dismutase (SOD-I), Mn-SOD (SOD-II) and glutathione peroxidase (GPx1-c-Myc-tagged) [2-4]. PASMC were infected with five plaque-forming units per cell in medium for 18 hrs and then changed to complete medium without virus. Experiments were performed 36 to 48 hrs after infection.

Pulmonary microvessel myocyte isolation. PASMC were isolated from rat lungs as described previously [5] using a modification of the method of Marshall et al. [6]. Cells isolated by this method were confirmed to be PASMC as previously described [5].

Measurements of GSH and GSSG. GSH and GSSG were measured in PASMC using a Bioxytech GSH/GSSG-412 kit (Oxis Health Products, Inc). Briefly, PASMC were grown to confluence in 100 mm dishes and incubated at 37°C in a hypoxic glove-box (1.5% O₂, 5% CO₂, balance N₂, Coy Instruments) or in a standard incubator exposed to room air with 5% CO₂ (normoxic) for 2 hrs. Other dishes were treated with H₂O₂ (20 μmol/L) for 15 min under normoxic conditions. At the conclusion of the treatment, the

media was removed and the dishes were chilled to 0°C. Cells were scraped down into the residual media (200-400 μ L), which was collected and stored at -70° C. The samples were then assayed according to the manufacturer's recommendations and the results calculated as the GSH:GSSH ratio.

Western blotting. PASMC were washed with PBS, then lysed with buffer (Tris (50 mmol/L), NaCl (150 mmol/L), SDS (0.1%), EDTA (5 mmol/L), β -glycerophosphate (18.5 mmol/L)) containing freshly added protease inhibitor cocktail (Roche), PMSF (1 mmol/L), sodium fluoride (10 mmol/L), and sodium orthovanadate (250 μ mol/L). Cell extracts were vortexed, incubated on ice for 20 min, centrifuged at 16,000xg for 20 min, and the supernatant was stored at -70° C. Protein extracts were electrophoresed using SDS-PAGE, and transferred to a nitrocellulose membrane. Membranes were blocked with TBS+0.1% Tween-20 (TBS-T) + 5% nonfat milk. Primary antibodies against SOD-I, SOD-II (Stressgen), catalase (Abcam), or c-Myc (GPx1; Santa Cruz Biotechnology, Inc) were added to TBS-T+5% milk+ 0.01% azide and incubated with the membrane overnight at 4° C. Membranes were washed with TBS-T, and secondary antibodies conjugated with HRP were added for 2 hr. Membranes were washed with TBS-T, stained with ECL reagent (Amersham), and exposed to film.

Immunocytochemistry. PASMC were cultured on glass cover slips until 75% confluent. Cells were then washed with PBS and fixed in 3% paraformaldehyde/0.02% glutaraldehyde in PBS. Cells were permeabilized by immersion in methanol (-20° C, 10 sec), then incubated in NaBH₄ (0.5 mg/ml, 3x, 15 min) followed by multiple washes. After blockade in normal goat serum (1%), cells were incubated with primary antibodies (60 min), washed, incubated with secondary antibodies labeled with ALEXA660 (60

min) and washed again. Images were then obtained using a laser scanning confocal microscope.

FRET probes. The HSP-FRET probe was generated by inserting YFP into the pECFP-N1 plasmid (Clontech) between the NheI and Bgl II sites, and then ligating the redox-sensitive regulatory domain from the E. coli HSP-33 between YFP and CFP via the EcoRI and BamHI sites [7]. Cells were placed into suspension by trypsinization, then transfected with HSP-FRET using an Amaxa Nucleofector device and plated on glass cover slips. HSP-FRET was excited at 430 nm, while fluorescence emission images were obtained at 470 nm (FRET donor, CFP) and 535 (FRET acceptor, YFP) to measure cell redox. Under reducing conditions the CFP and YFP are in close proximity, and FRET is high. During oxidant stress, oxidation of thiols in the HSP-33 regulatory domain separates the fluorophores and decreases FRET. This increases image intensity at 470 and decreases intensity at 535 nm, resulting in an increase in the 470/535 HSP-FRET ratio. When expressed in the cytosol, HSP-FRET responds in a dose-dependent manner to exogenous H_2O_2 but does not respond to exogenous nitric oxide [7].

A genetically-encoded FRET-based sensor was used to measure $[Ca^{2+}]_i$. YC2.3 is a high affinity Ca^{2+} sensor, consisting of CFP and citrine, a mutant of YFP linked by a calmodulin-M13 hinge region (plasmid encoding YC2.3 was provided by Dr. R.Y. Tsien, Howard Hughes Medical Institute, University of California at San Diego) [8-10]. When bound to Ca^{2+} , FRET between CFP and citrine increases. An increase in $[Ca^{2+}]_i$ is reflected by an increase in the citrine/CFP intensity ratio (535/470). The YC2.3 probe was determined to be unresponsive to exogenously applied oxidants (see Online Supplement data). YC2.3 was packaged in a recombinant adenovirus to permit efficient

expression of the probe in PASMC.

After allowing 24 hr for expression of either of these sensors, PASMC plated on glass cover slips were placed in a flow-through chamber mounted on an inverted microscope. Imaging data acquisition and analysis were accomplished using MetaMorph/MetaFluor software (Universal Imaging Corp.). Cells were primed by addition of endothelin-1 (ET-1, 1 nmol/L) beginning 10 min prior to and during hypoxia [11, 12]. Changes in FRET image ratio in response to ET-1 were minor, and returned to baseline before the hypoxic challenge. Images containing 2-8 cells were collected 1-5 times each minute. FRET emission ratios were normalized to baseline values at the end of 15 min of normoxic equilibration. Normoxic cells were perfused with a balanced salt solution bubbled with a 21% O₂, 5% CO₂, 74% N₂ gas. Hypoxia was induced by bubbling with a 0-1% O₂, 5% CO₂, 96% N₂ gas.

Simultaneous measurements of [Ca²⁺]_i and ROS levels were performed using a method similar to one previously described [13, 14]. Briefly, spectral separation of HSP-FRET and Fura-2 excitation and emission permits simultaneous imaging of ROS signaling and [Ca²⁺]_i in single cells. PASMC were cells transiently transfected with HSP-FRET. After allowing 24 hr for expression, the cells were loaded with Fura-2 acetoxymethyl ester (5 μmol/L; Molecular Probes, Inc.) for 1 hr and then incubated for an additional 15 min in medium without the dye to allow for de-esterification of the intracellular dye. **Images were obtained every 20 seconds. First, HSP-FRET was excited at 430 nm, while fluorescence emission images were obtained at 470 nm (FRET donor, CFP) and 535 (FRET acceptor, YFP) to assess cellular redox. This was followed immediately by excitation at 340 and 380 nm, and emission at 530 nm, in order to assess**

$[Ca^{2+}]_i$ using Fura-2 ratios. A 455-nm dichroic filter was used for HSP-FRET and Fura-2. Results are expressed as the ratio of FRET donor and acceptor emission (470/535 nm ratio) and the Fura-2 340 and 380 nm excitation (340/380 nm ratio) normalized to the normoxic baseline values prior to the start of hypoxia. The data presented is an average of the HSP-FRET and Fura-2 ratios for 4 cover slips containing 4-8 cells each.

Statistics. ANOVA was used to identify significant differences between groups. To control for differences in the hypoxic responses of cultured myocytes, experimental studies and control experiments were always carried out on the same day. Statistical significance was set at P<.05 [15].

Additional Figures

Online Figure 1. Laser scanning confocal images detailing expression of the A-C) HSP-FRET probe and D-F) EGFP-N1 in PASMC. Confocal microscopy was performed to compare the distribution of HSP-FRET with that of a commercially obtained, non-targeted, GFP expression vector (Clontech EGFP-N1) in PASMC. The nuclei were stained with DAPI and mitochondria were counter-stained using Mitotracker Red. Cell images of HSP-FRET were obtained using excitation laser line at 488 nm and emission at 535 nm. There is no observable difference in the cellular expression pattern between the HSP-FRET probe and the commercially available EGFP-N1 by confocal microscopy. Both showed expression in the cytosol with some overlap with the nucleus. **G) PASMC expressing either HSP-FRET or YC2.3 were excited at 430 nm, while fluorescence emission images were obtained at 470 nm (FRET donor, CFP) and 535 (FRET acceptor,**

YFP). CFP and YFP images were then overlaid in order to verify co-localization of the fluorophores in the cell.

Online Figure 2. Control studies for the HSP-FRET probe expressed in PASMC. 2A) Experiments were performed to assess the effect of PDTC, NAC, or CN- alone on the HSP-FRET ratio during normoxia. PASMC expressing the HSP-FRET probe were superfused with normoxic media to establish a baseline. Experimental agents were added and HSP-FRET measurements were continued. In separate experiments, PASMC expressing the HSP-FRET probe were challenged with hypoxia (1.5% O₂) for comparison. None of these agents had an effect on baseline HSP-FRET ratio. Moreover, in studies using the HSP-FRET probe, the pharmacological agents myxothiazol, cyanide, PDTC or NAC were administered during a 10-minute pre-incubation period before the onset of hypoxia. None of these agents affected the baseline ratios during this time period (data not shown). 2B) Experiments were performed to determine the effect of acidosis on the HSP-FRET ratio. PASMC expressing the HSP-FRET probe were superfused with normoxic media to establish a baseline. The gas bubbling the media superfusing the cells was switched from 5 to 20% and HSP-FRET measurements were continued. In separate experiments, PASMC expressing the HSP-FRET probe were challenged with hypoxia (1.5% O₂) for comparison. A small increase in the HSP-FRET ratio was observed when CO₂ was changed from 5 to 20%, although this did not reach statistical significance. Such an increase in CO₂ should have caused a significant decrease in intracellular pH, of a magnitude expected during ischemia. However, the PASMC in the present sets of studies were never subjected to ischemia, and the CO₂ was

maintained at physiological levels by superfusion with buffer equilibrated with 5% CO₂. We therefore conclude that the significant increase in HSP-FRET ratio observed during hypoxia was most likely due to oxidant signaling.

Online Figure 3. Control studies for the YC2.3 probe expressed in PASMC. 3A) Experiments were performed to determine if the YC2.3 probe was sensitive to oxidative stress. PASMC expressing the YC2.3 probe were depleted of intracellular calcium with thapsigargin (20 nM) and superfused with Ca²⁺-free, normoxic media to establish a baseline. H₂O₂ at 50 and 100 μM were added to the media superfusing the PASMC and measurements were continued. In separate experiments, PASMC expressing the YC2.3 probe were challenged with Ca²⁺-containing hypoxia (1.5% O₂) media for comparison. There was no significant change in the baseline YC2.3 ratio when the cells were challenged with hydrogen peroxide, indicating that the YC2.3 is not sensitive to oxidant stress. 3B) Experiments were performed to assess the effect of PDTC or NAC alone on the YC2.3 ratio during normoxia. PASMC expressing the YC2.3 probe were superfused with normoxic media to establish a baseline. Experimental agents were added and YC2.3 measurements were continued. In separate experiments, PASMC expressing the YC2.3 probe were challenged with hypoxia (1.5% O₂) for comparison. None of these agents had an effect on baseline YC2.3 ratio. Moreover, in studies using the YC2.3 probe, the pharmacological agents myxothiazol, cyanide, PDTC or NAC were administered during a 10-minute pre-incubation period before the onset of hypoxia. None of these agents affected the baseline ratios during this time period (data not shown). 3C) Experiments were performed to determine if pharmacological as well as enzymatic antioxidants

affected the ability of the YC2.3 probe to detect an increase in cytosolic calcium. PASMC were superfused with buffered-salt solution containing 5 mM Ca²⁺. When a baseline was established, the cells were challenged with 5 μ M A23187 to cause Ca²⁺ influx. The resulting change in YC2.3 ratio was similar to the hypoxia-induced change. PASMC pretreated with NAC, PDTC, or overexpressing GPx1 or mitochondrial catalase, did not lose the ability of YC2.3 to detect an A23187-induced increase in cytosolic calcium. These findings show that YC2.3 can still respond to calcium changes in the presence of antioxidants or antioxidant enzymes.

Online Figure 4. Determining if co-expression of the cytosolic and mitochondrial catalase further attenuates the hypoxia-induced increase in HSP-FRET and YC2.3 ratios. Experiments were performed addressing the effect of the co-expression of cytosolic and mitochondrial catalase on both the hypoxia-induced increases in HSP-FRET and YC2.3 responses. There was no significant additive effect when we co-expressed these agents, compared to the individual effects of these agents alone.

Online Figure 5. Determining whether myxothiazol attenuates the hypoxia-induced increase in cytosolic calcium in SOD-II overexpressing cells. 10 μ mol/L Myxothiazol significantly attenuated the hypoxia-induced increase in YC2.3 ratio in cells overexpressing SOD-II. This result further supports our hypothesis that complex III is the source of increased superoxide generation during hypoxia, which is then dismuted into H₂O₂ by SOD-II overexpression, resulting in an increase in cytosolic calcium signaling.

Online Figure 6. Determining the effect of cyanide on hypoxia-induced ROS and cytosolic calcium signals in the presence of myxothiazol. 10 μ mol/L Myxothiazol significantly attenuated the cyanide-induced increases in ROS and cytosolic calcium signaling during hypoxia. These results further support our hypothesis that complex III is the source of the ROS signal during hypoxia.

References

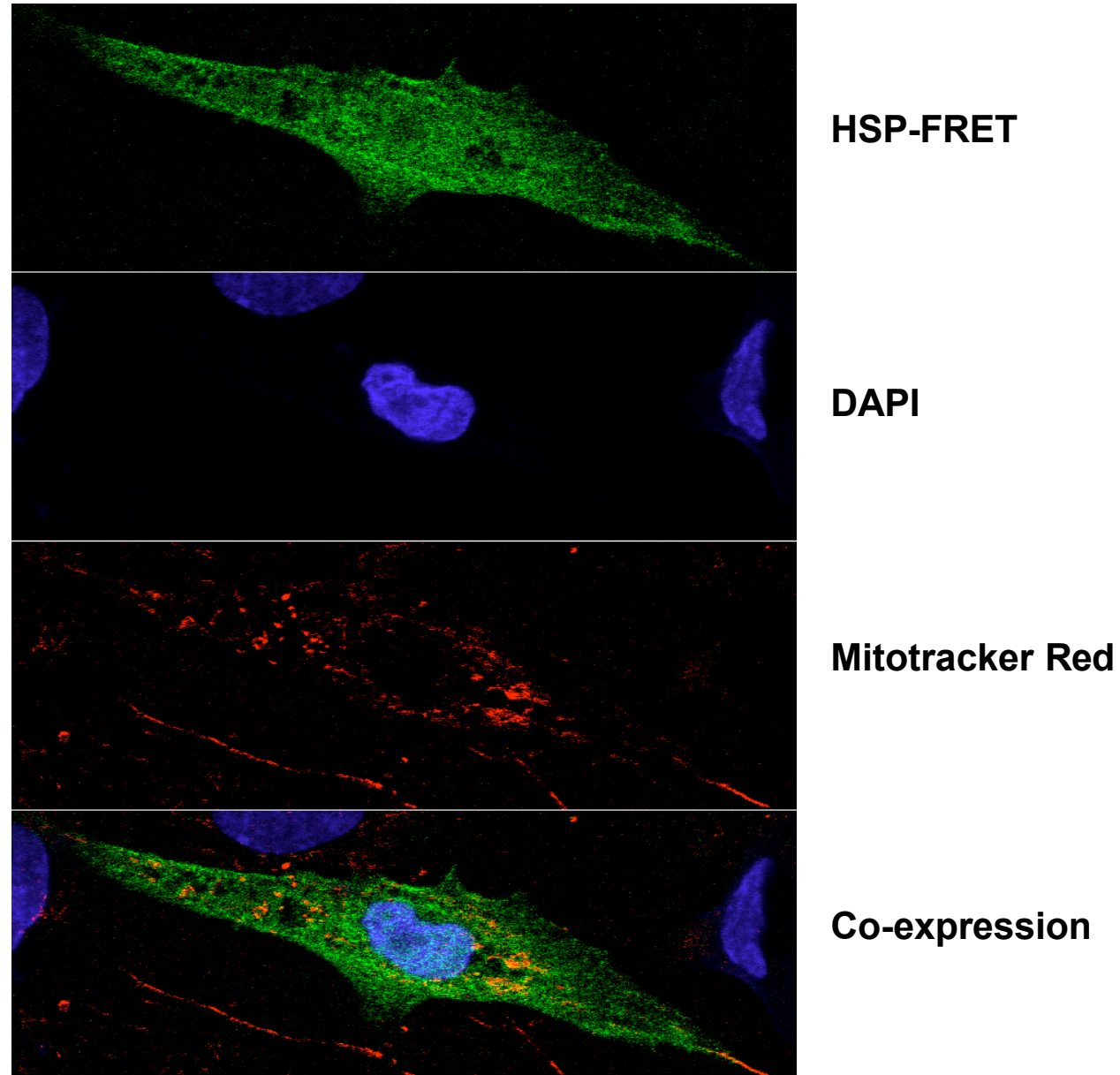
1. Bai J and Cederbaum AI. Overexpression of catalase in the mitochondrial or cytosolic compartment increases sensitivity of HepG2 cells to tumor necrosis factor-alpha-induced apoptosis. *J Biol Chem.* 2000;275:19241-9.
2. Zwacka RM, Zhou W, Zhang Y, Darby CJ, Dudus L, Halldorson J, Oberley L, Engelhardt JF. Redox gene therapy for ischemia/reperfusion injury of the liver reduces AP1 and NF-kappaB activation. *Nat Med.* 1998;4:698-704.
3. Zwacka RM, Dudus L, Epperly MW, Greenberger JS, Engelhardt JF. Redox gene therapy protects human IB-3 lung epithelial cells against ionizing radiation-induced apoptosis. *Hum Gene Ther.* 1998;9:1381-6.
4. Li Q, Sanlioglu S, Li S, Ritchie T, Oberley L, Engelhardt JF. GPx-1 gene delivery modulates NFkappaB activation following diverse environmental injuries through a specific subunit of the IKK complex. *Antioxid Redox Signal.* 2001;3:415-32.

5. Waypa GB, Chandel NS, Schumacker PT. Model for hypoxic pulmonary vasoconstriction involving mitochondrial oxygen sensing. *Circ Res.* 2001;88:1259-66.
6. Marshall C, Mamary AJ, Verhoeven AJ, Marshall BE. Pulmonary artery NADPH-oxidase is activated in hypoxic pulmonary vasoconstriction. *Am J Respir Cell Mol Biol.* 1996;15:633-44.
7. Guzy RD, Hoyos B, Robin E, Chen H, Liu L, Mansfield KD, Simon MC, Hammerling U, Schumacker PT. Mitochondrial complex III is required for hypoxia-induced ROS production and cellular oxygen sensing. *Cell Metab.* 2005;1:401-8.
8. Miyawaki A, Llopis J, Heim R, McCaffery JM, Adams JA, Ikura M, Tsien RY. Fluorescent indicators for Ca²⁺ based on green fluorescent proteins and calmodulin. *Nature.* 1997;388:882-7.
9. Miyawaki A, Griesbeck O, Heim R, Tsien RY. Dynamic and quantitative Ca²⁺ measurements using improved cameleons. *Proc Natl Acad Sci U S A.* 1999;96:2135-40.
10. Griesbeck O, Baird GS, Campbell RE, Zacharias DA, Tsien RY. Reducing the environmental sensitivity of yellow fluorescent protein. Mechanism and applications. *J Biol Chem.* 2001;276:29188-94.
11. McMurtry IF. Angiotensin is not required for hypoxic constriction in salt solution-perfused rat lungs. *J Appl Physiol.* 1984;56:375-80.

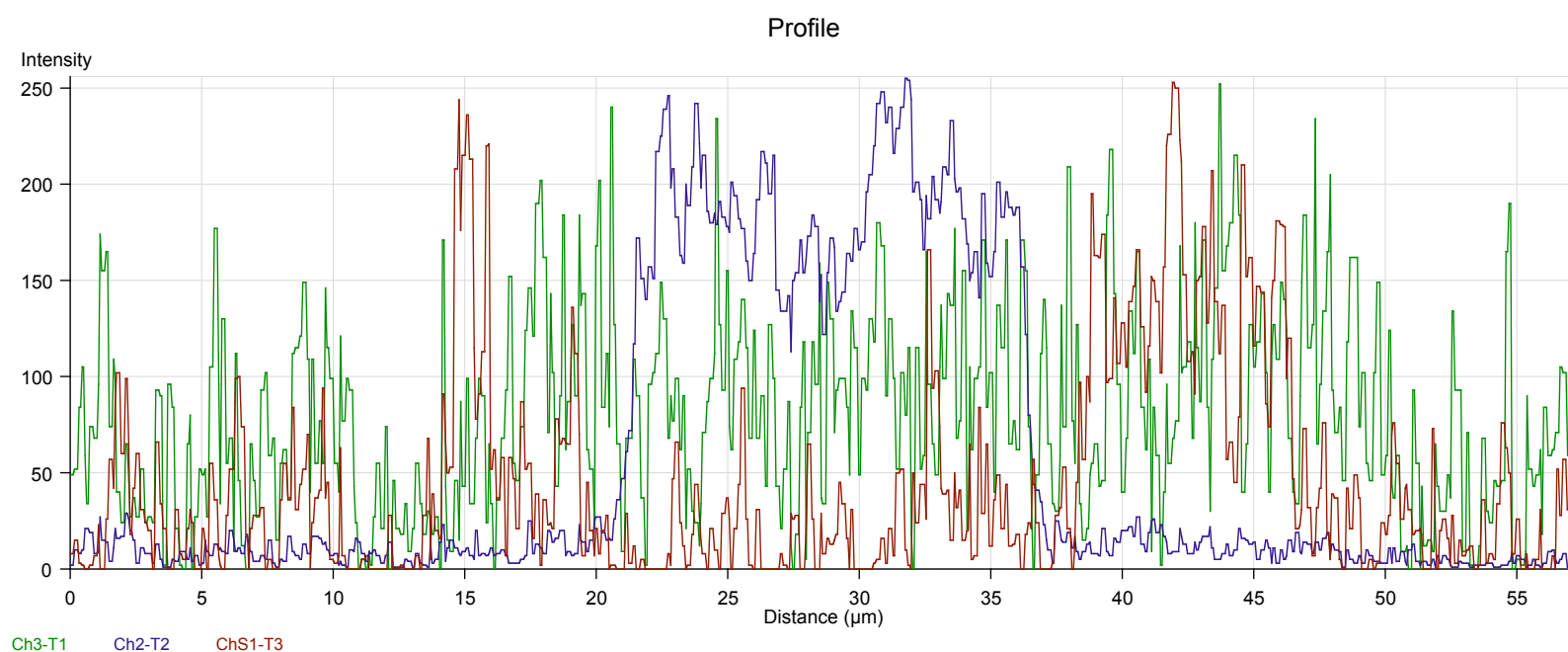
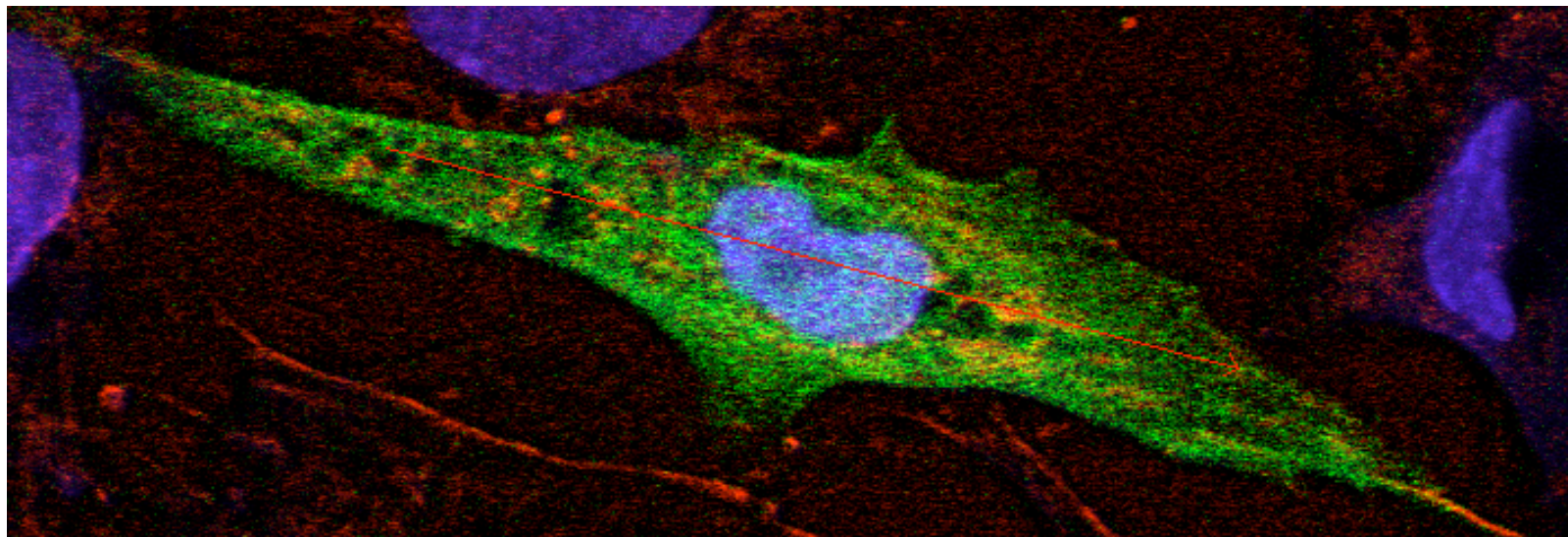
12. Liu Q, Sham JS, Shimoda LA, Sylvester JT. Hypoxic constriction of porcine distal pulmonary arteries: endothelium and endothelin dependence. *Am J Physiol Lung Cell Mol Physiol*. 2001;280:L856-65.
13. Landa LR, Jr., Harbeck M, Kaihara K, Chepurny O, Kitiphongspattana K, Graf O, Nikolaev VO, Lohse MJ, Holz GG, Roe MW. Interplay of Ca²⁺ and cAMP signaling in the insulin-secreting MIN6 beta-cell line. *J Biol Chem*. 2005;280:31294-302.
14. Palmer AE, Jin C, Reed JC, Tsien RY. Bcl-2-mediated alterations in endoplasmic reticulum Ca²⁺ analyzed with an improved genetically encoded fluorescent sensor. *Proc Natl Acad Sci U S A*. 2004;101:17404-9.
15. Wallenstein S, Zucker CL, Fleiss JL. Some statistical methods useful in circulation research. *Circ Res*. 1980;47:1-9.

OnlineFigure 1A.

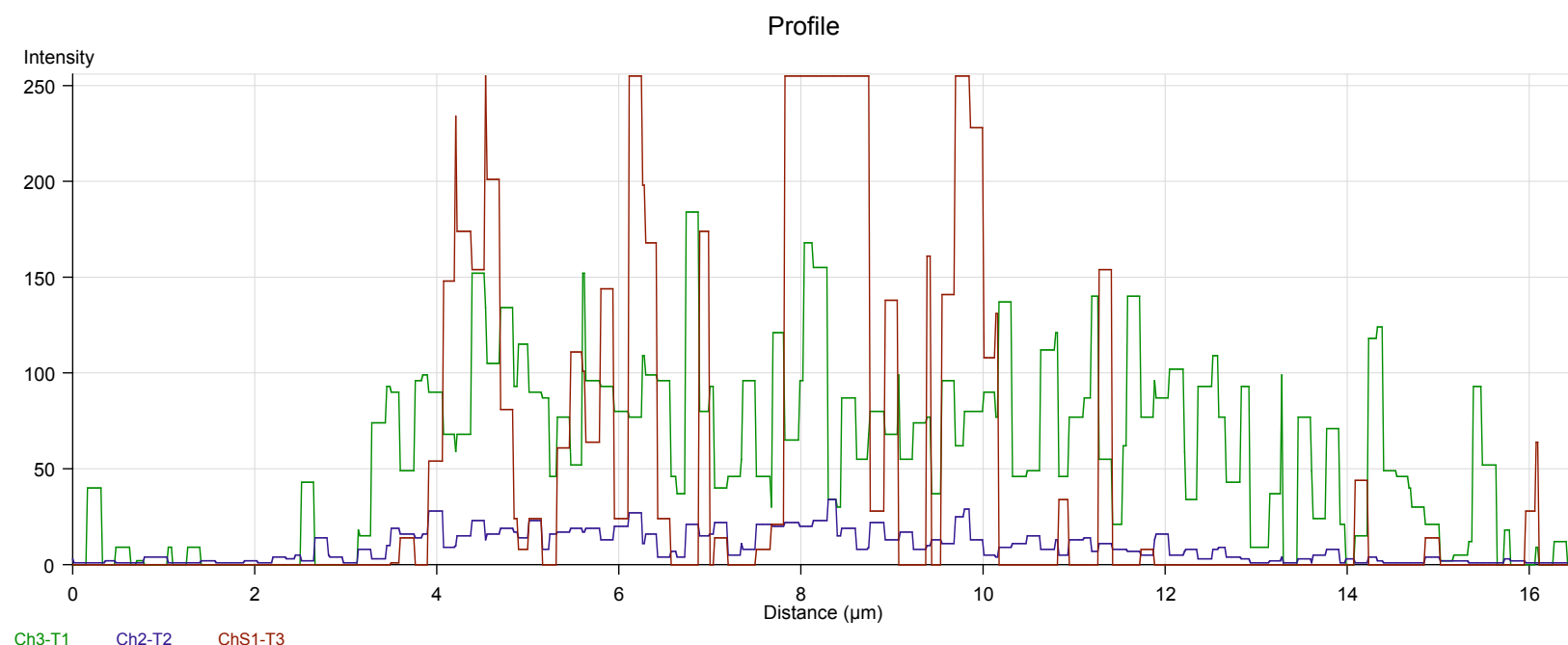
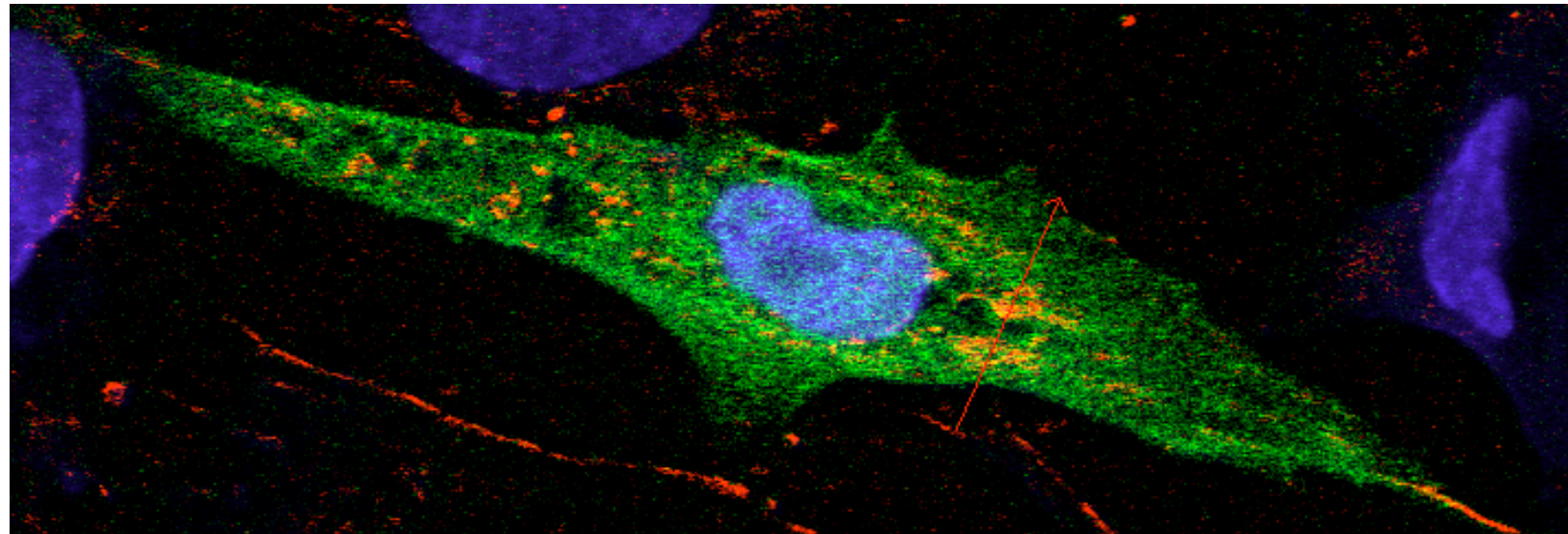
PA Myocyte: HSP-FRET, DAPI, Mitotracker Red.



Online Figure 1B. PA Myocyte: HSP-FRET, DAPI, Mitotracker Red.

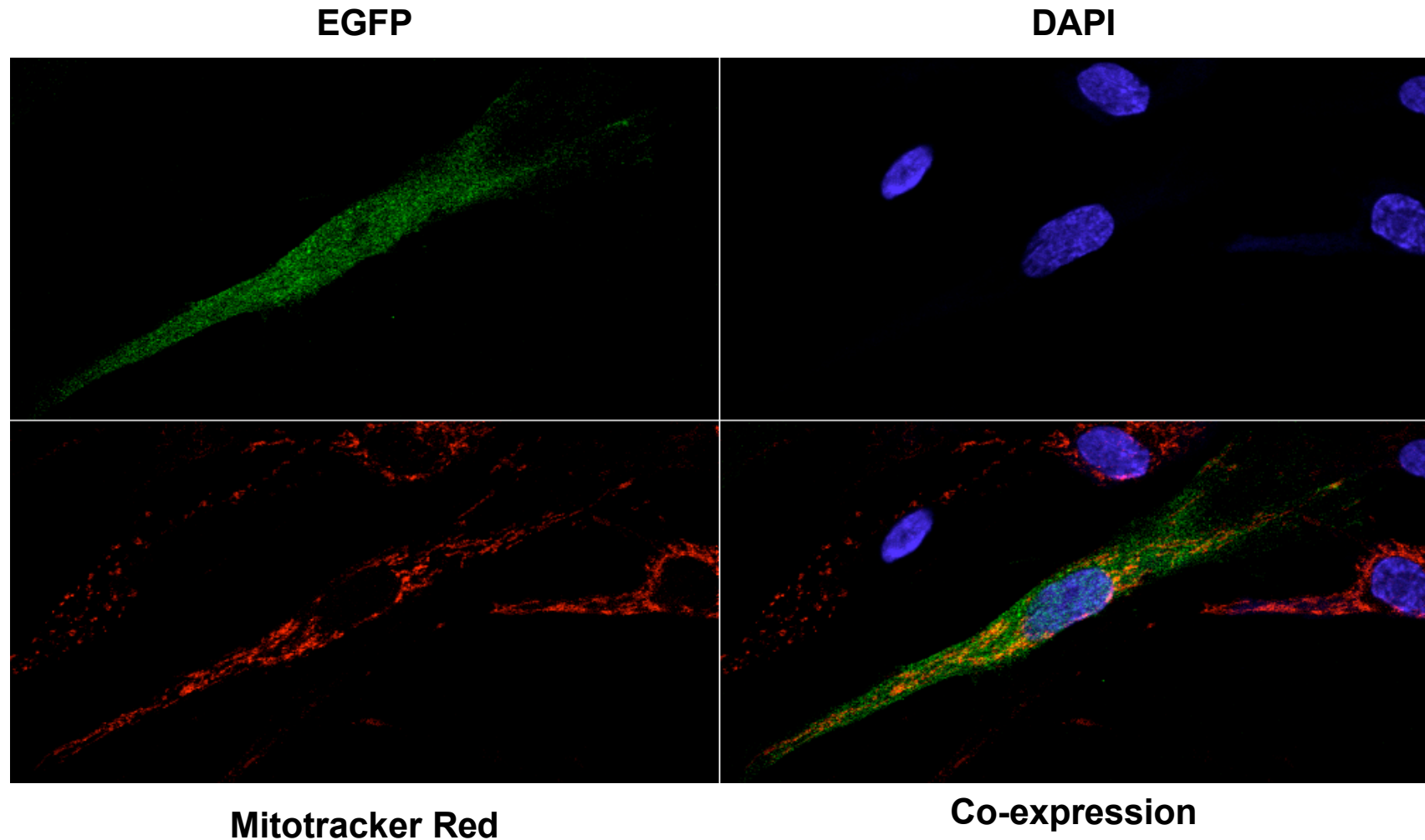


Online Figure 1C. PA Myocyte: HSP-FRET, DAPI, Mitotracker Red.



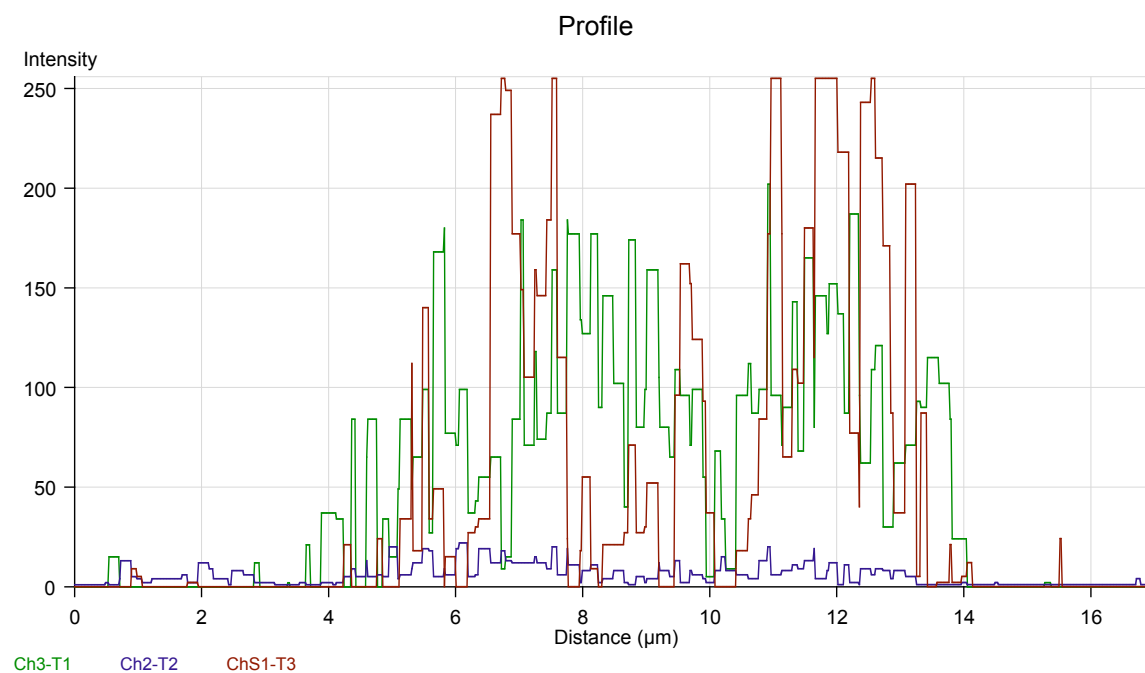
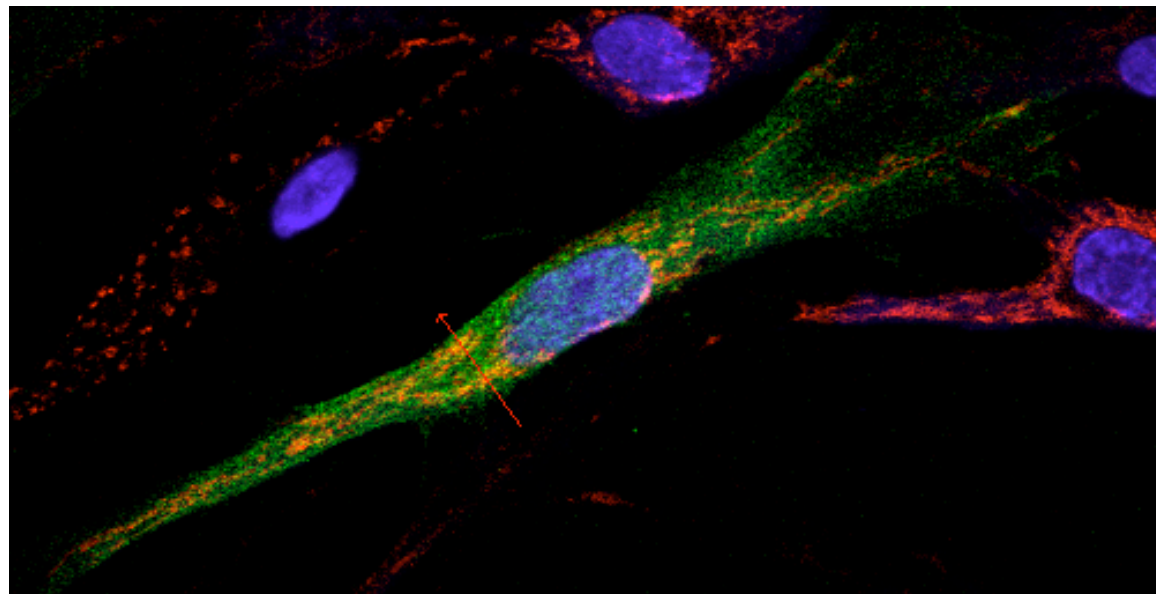
Online Figure 1D.

PA Myocyte: EGFP, DAPI, Mitotracker Red.



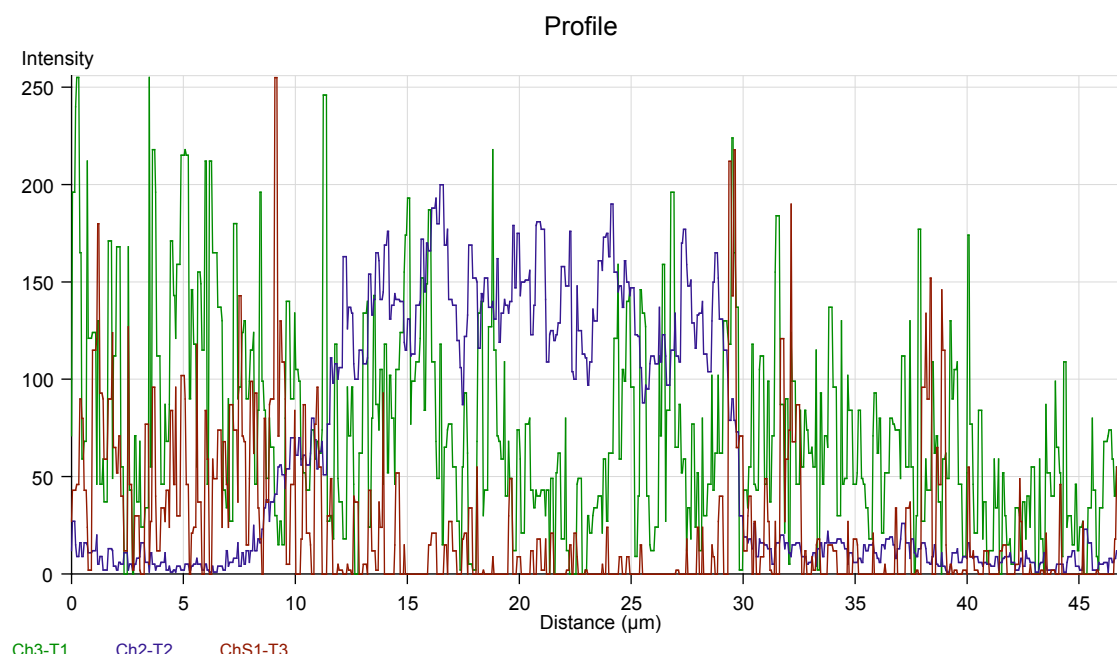
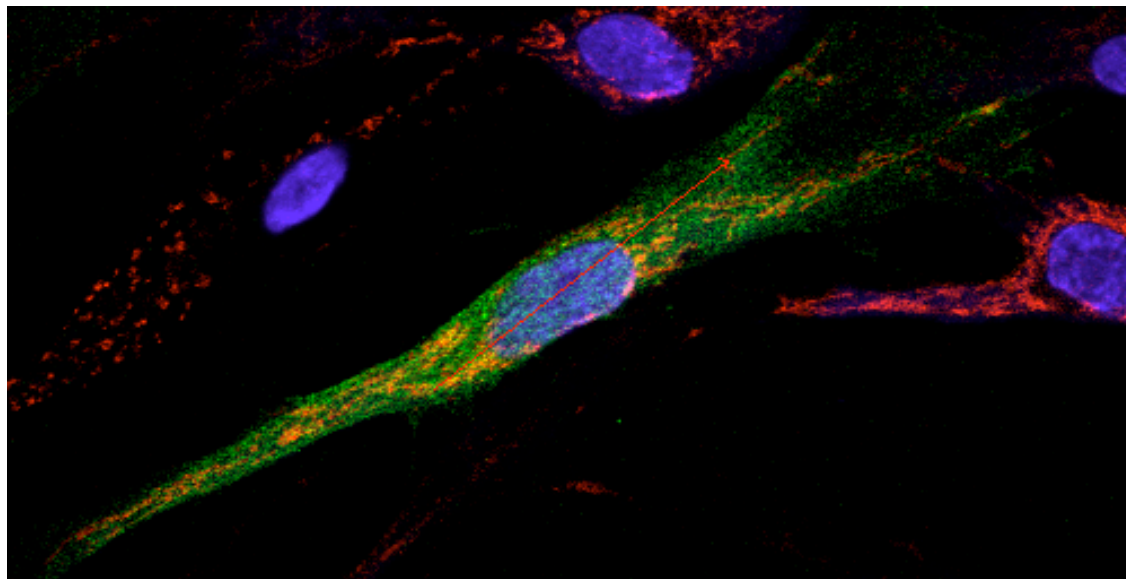
Online Figure 1E.

PA Myocyte: EGFP, DAPI, Mitotracker Red.



Online Figure 1F.

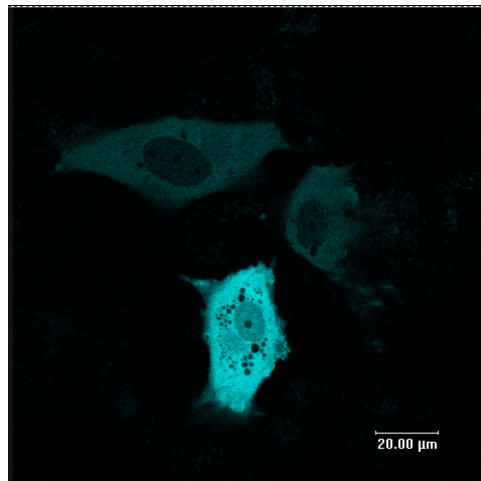
PA Myocyte: EGFP, DAPI, Mitotracker Red.



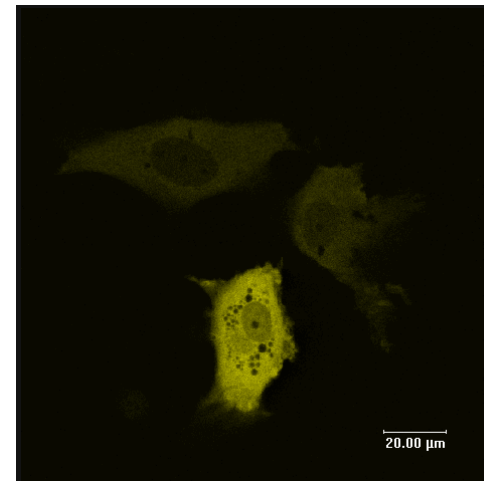
Online Figure 1G.

HSP-FRET

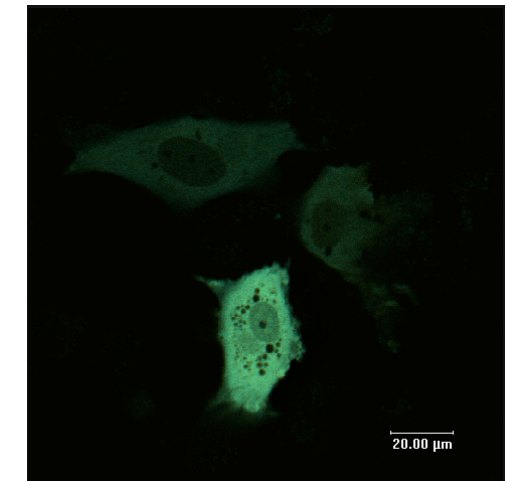
CFP Fluorescence



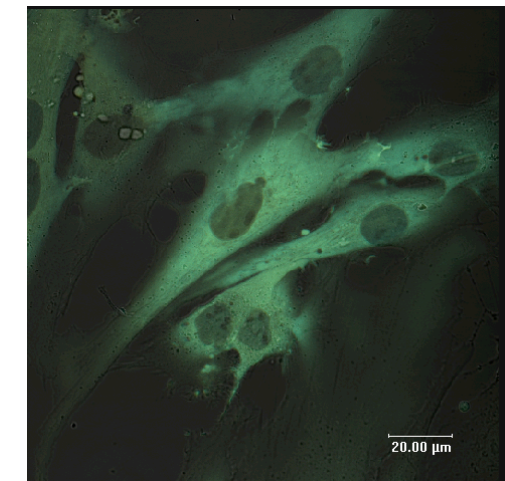
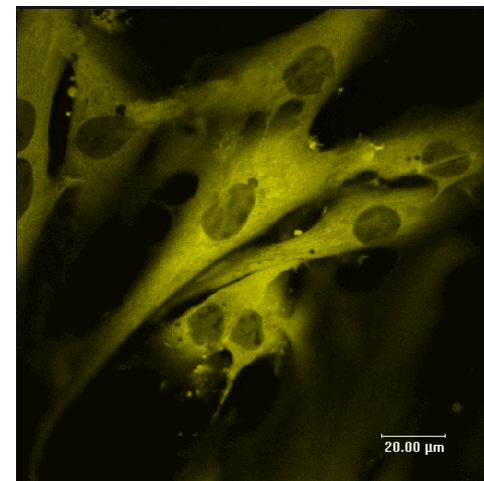
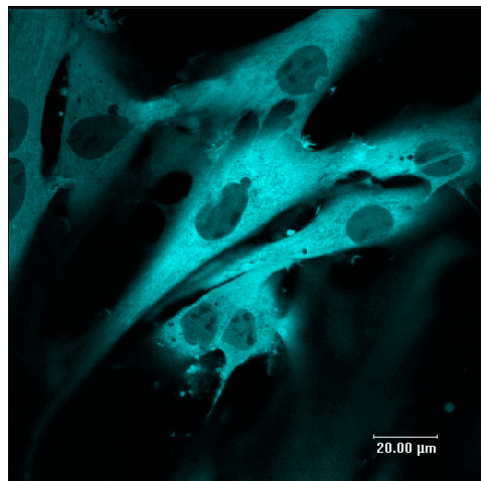
YFP Fluorescence



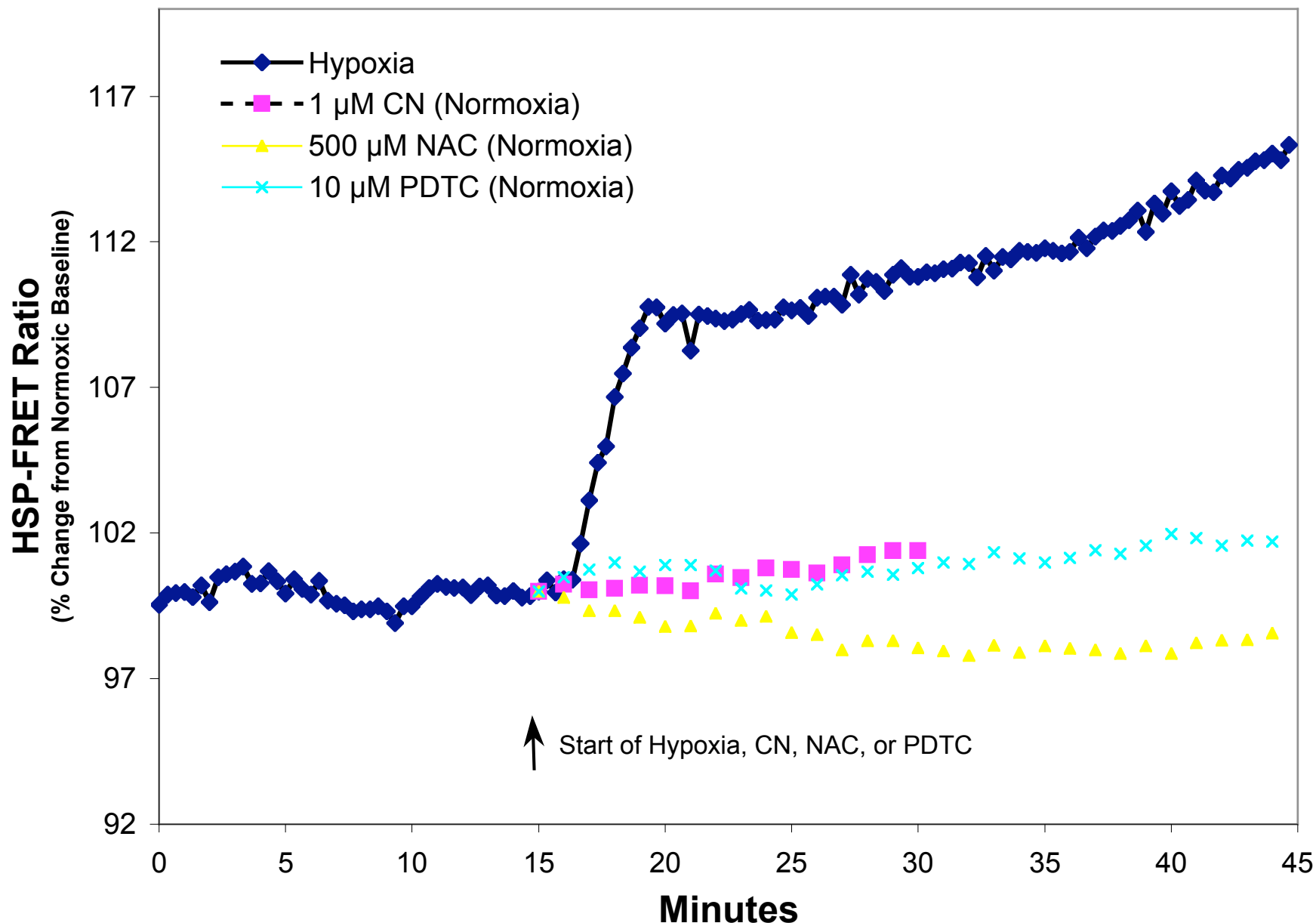
CFP/YFP Co-localization



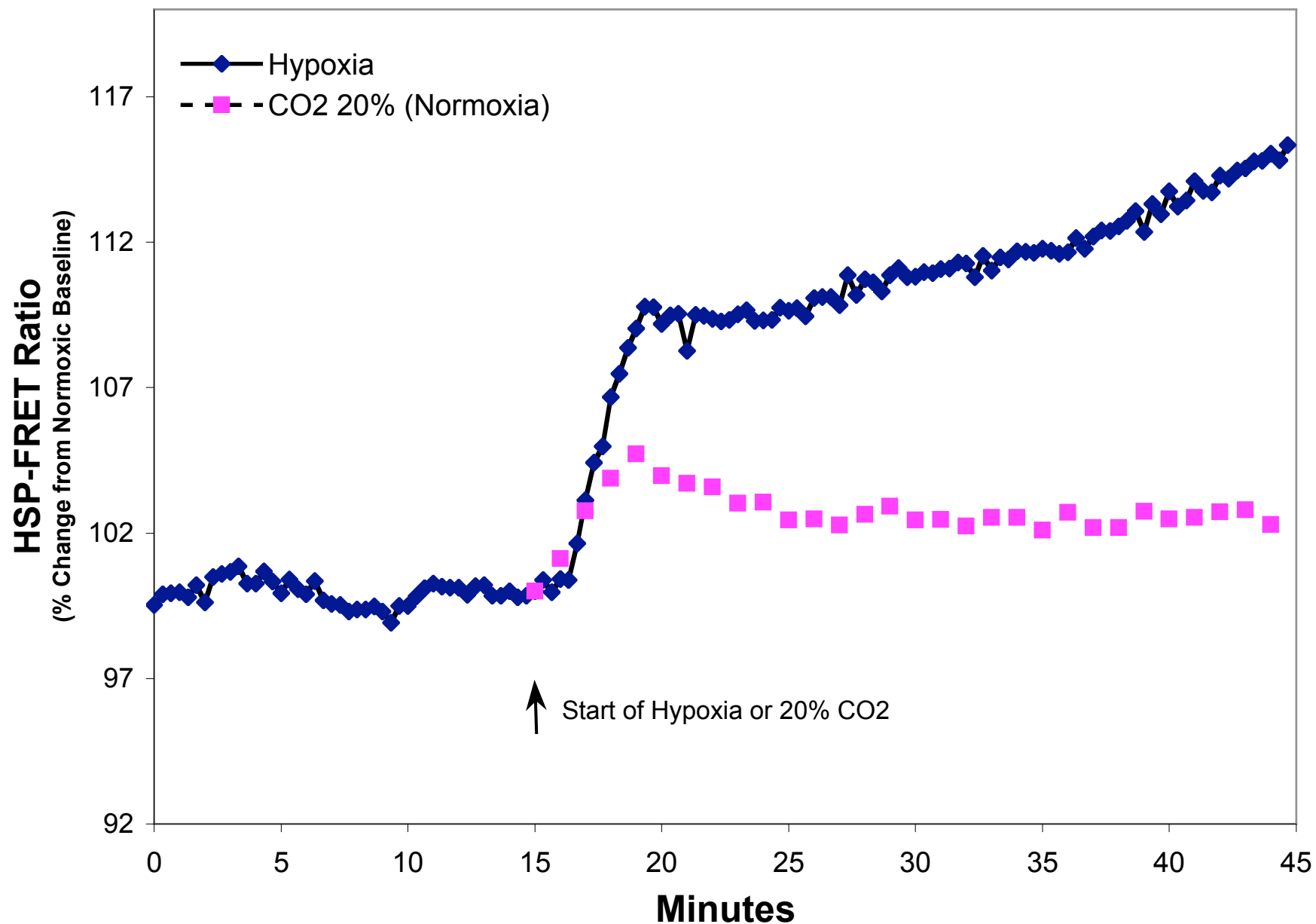
YC2.3



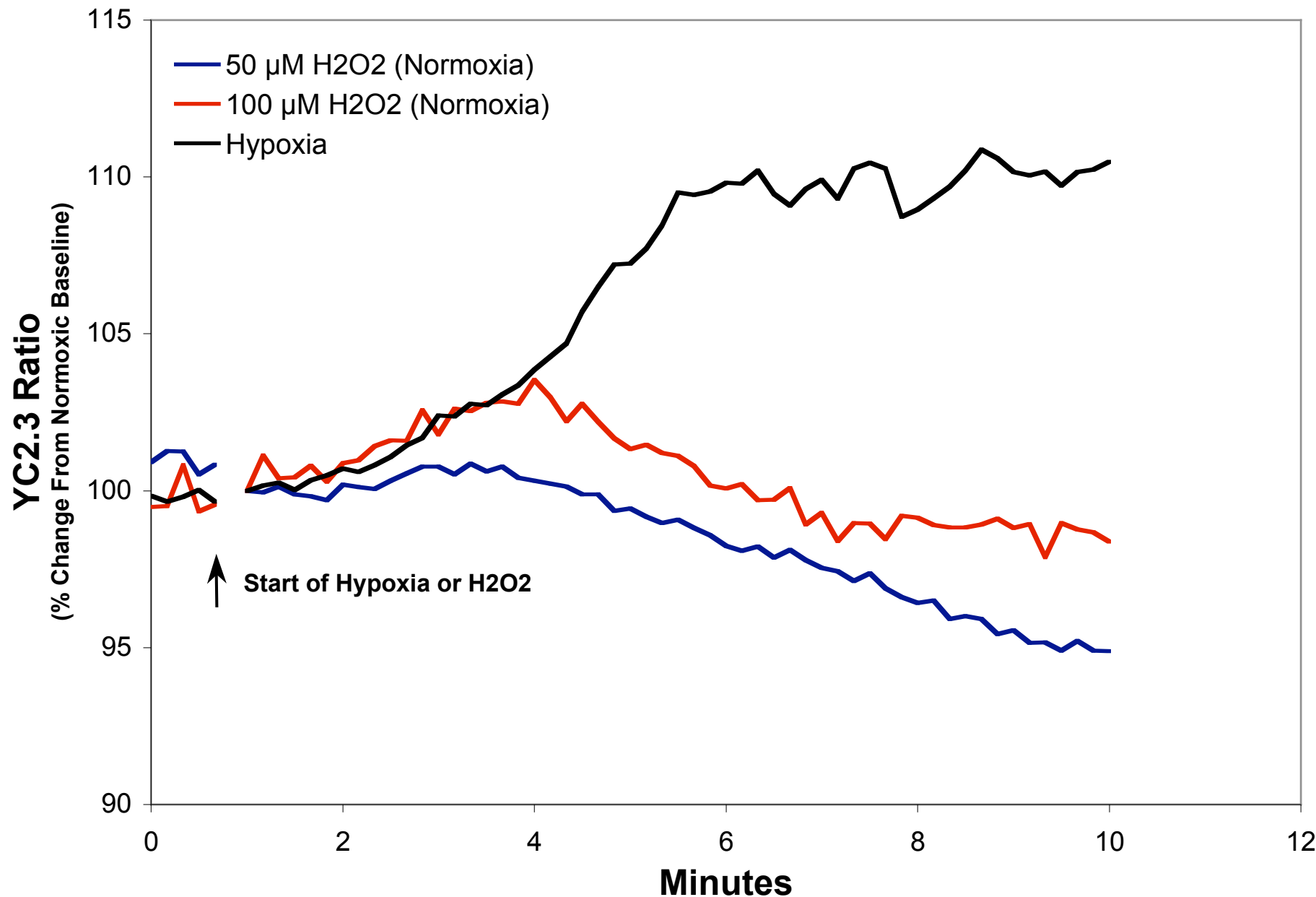
Online Figure 2A.



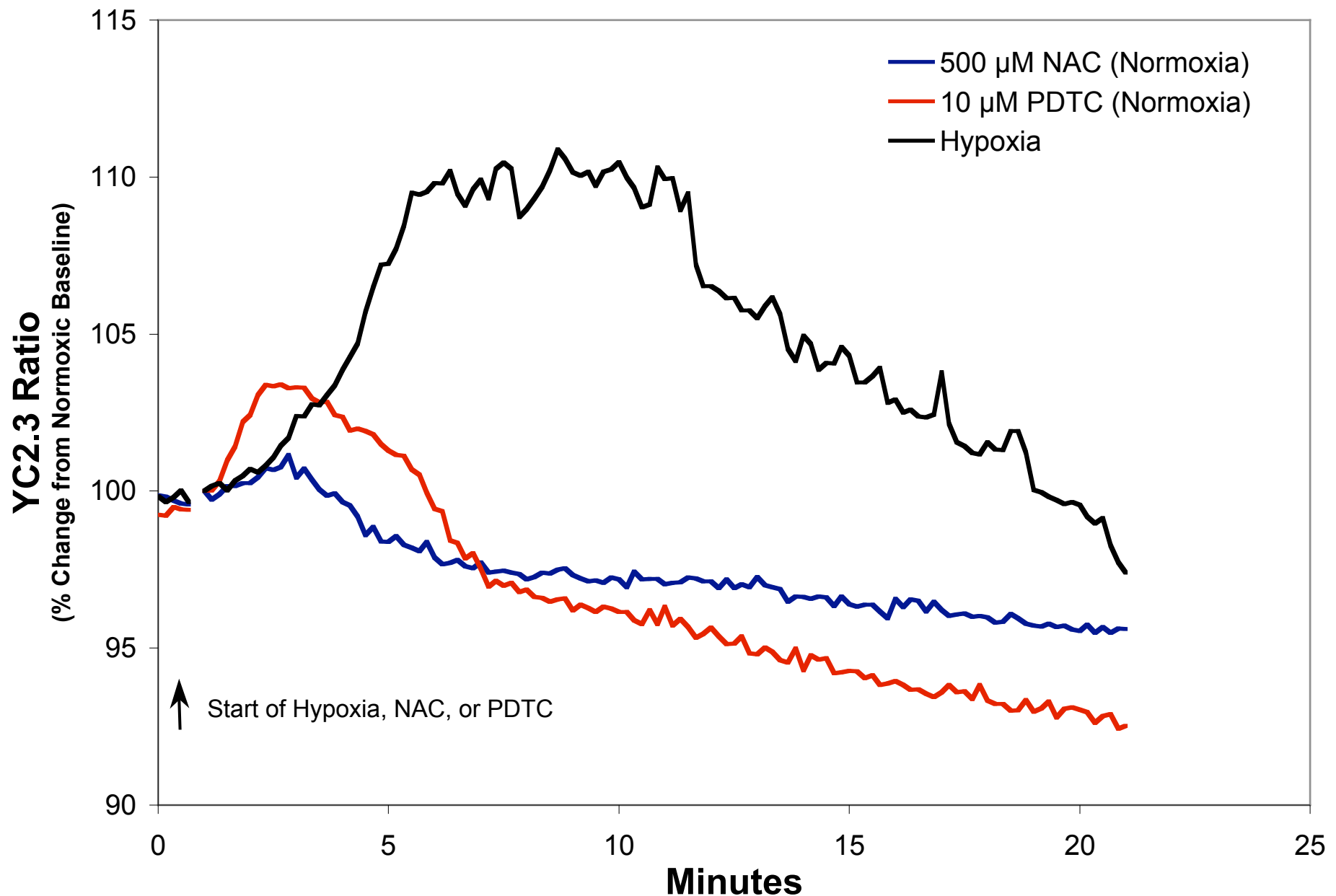
Online Figure 2B.



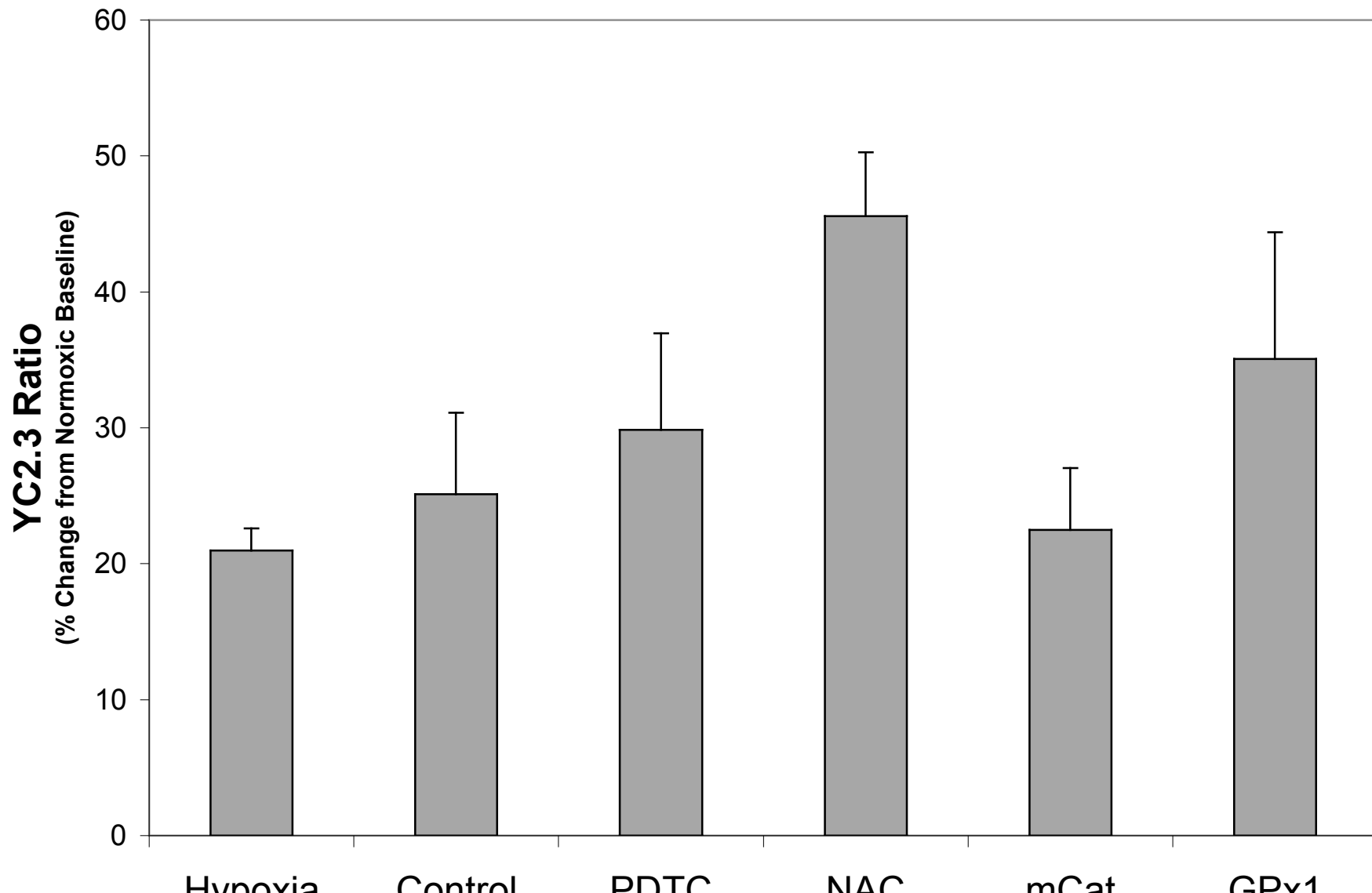
Online Figure 3A.



Online Figure 3B.

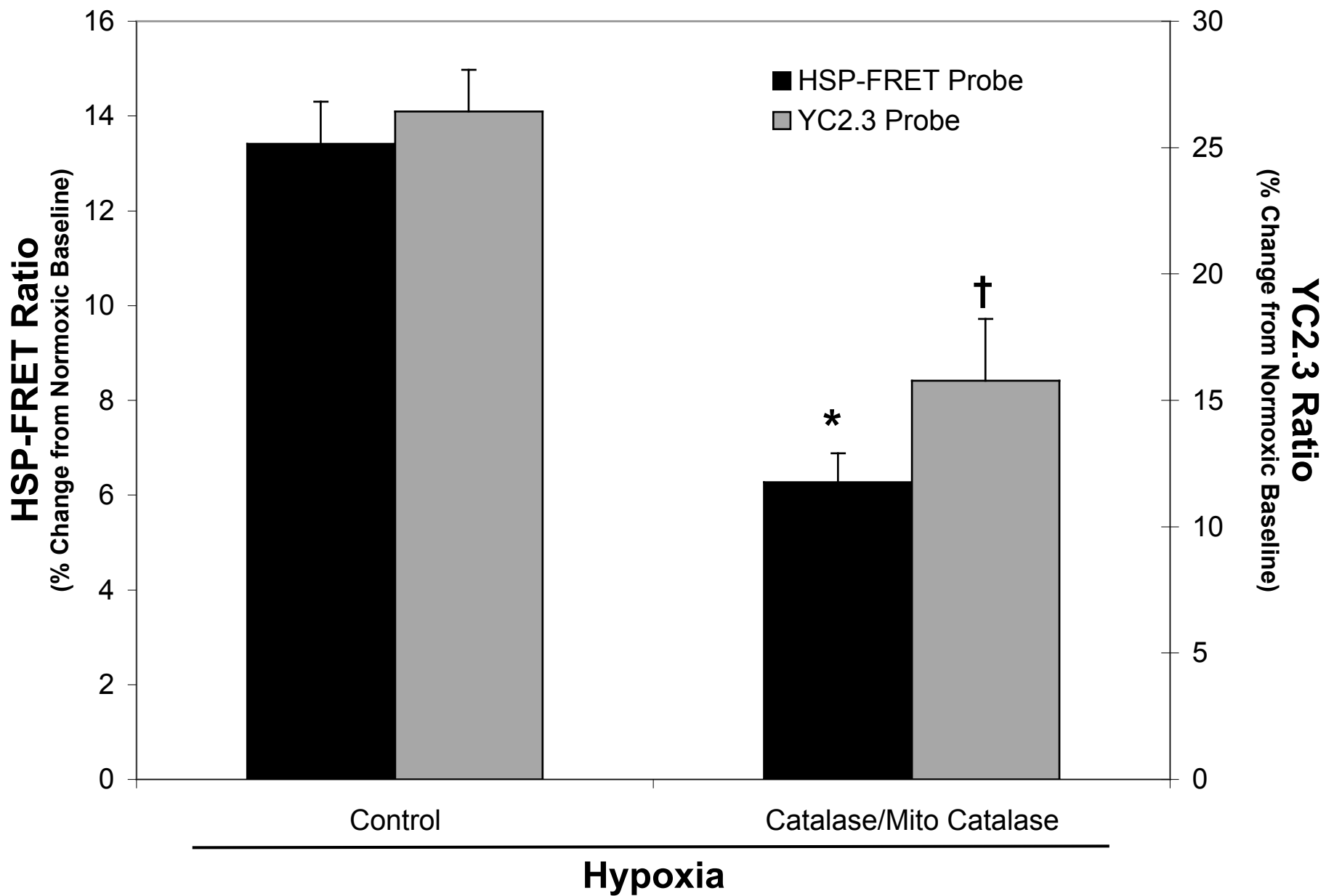


Online Figure 3C.

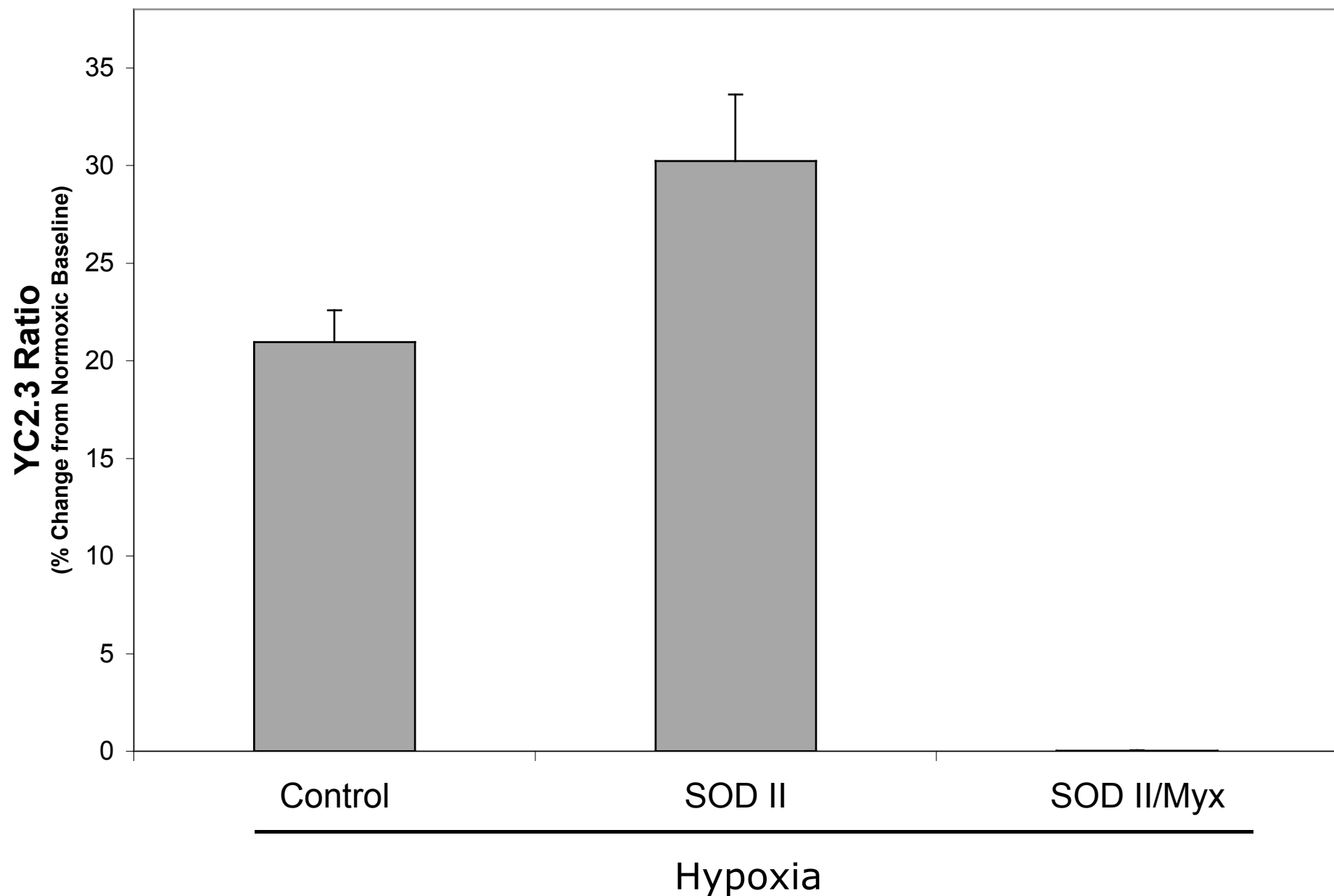


A23187

Online Figure 4.



Online Figure 5.



Online Figure 6.

